Horizon 2020

Project acronym: **LASH FIRE**

Project full title: **Legislative Assessment for Safety Hazard of Fire and Innovations in Ro-ro ship Environment**

Grant Agreement No: **814975**

Coordinator: **RISE Research Institutes of Sweden**

Deliverable D11.1

Development, theoretical evaluation and preliminary assessment of requirements for horizontal division of ro-ro spaces

February 2022

Dissemination level: **Public**

Abstract

The International Maritime Organization, through its correspondence group on fire safety, has underlined the need for more scientific studies regarding the performance of A-60 boundaries in case of a ro-ro space fire. The goal of the present study was to clarify the state-of-the-art fire protection capacity of A class thermal insulation when exposed to the heat exposure from a realistic fire in a ro-ro space. The study has been conducted in Work Package 11 - Containment (WP11) of the EU funded project LASH FIRE.

The study started with determining the potential heat exposure to the ceiling during a fire within a ro-ro space. Representative scenarios defined were open and closed ro-ro spaces fully loaded with heavy goods vehicles (HGV), where the fire starts in one HGV. Determination of the possible heat exposure was conducted using two approaches. Fire tests of similar scenarios performed in previous projects were analysed and complemented with numerical simulations using Computational Fluid Dynamics (CFD). The temperatures were then compared with time-temperature curves for designing fire safety.

For most of the simulated scenarios (except the case of a closed ro-ro space with the ventilation turned off), the comparisons showed that the highest temperatures reached in the space fit better to the hydrocarbon time-temperature curve than the standard (cellulosic) time-temperature curve according to ISO 834 curve. As the hydrocarbon curve is more severe in terms of heat exposure than the standard time-temperature curve, used for type approval of thermal insulation, a set of experiments was carried out to expose A class thermal insulation to the hydrocarbon curve. For the tests, different thermal insulation (A-60 and A-30 based on glass wool and stone wool) were mounted on steel plates with different thicknesses (5 mm, 6 mm and 12 mm, respectively representing the thickness required by the Fire Test Procedures Code, the thickness of a steel plate designed for a deck dedicated for the storage of cars, and the thickness of a steel plate designed for a deck dedicated for the storage of trucks).

Tests results showed a significant reduction in fire integrity when exposed to the more severe hydrocarbon time-temperature curve. This reduction in fire integrity means a reduction in time to reach the maximum temperature elevation at the unexposed surface allowed by the Fire Tests Procedures Code (140 °C for the average temperature elevation and 180 °C for the highest temperature elevation). With thermal insulation of stone wool, the reduction was about 50% depending on the steel plate thickness. When exposed to the high heat exposure of the hydrocarbon curve, the thermal insulation based on glass wool showed a severe deterioration and then a very low fire integrity performance.

Based on the investigations made, the maritime community should be made aware that the current requirements do not provide a protection of 60 minutes (with A-60 thermal insulation) or 30 minutes (with A-30 thermal insulation). Depending on the steel plate thickness, the reduction in thermal insulation capacity was 45-60% of the values indicated by regulations, when exposed to a hydrocarbon heat exposure (realistic for most ro-ro spaces). If ship owners or shipbuilders really want to achieve 30 or 60 minutes of thermal insulation for a ro-ro space, they are recommended to assume a 50% reduction and use thermal insulation of a higher standard (e.g. A-60 instead of A-30) or use insulation type approved with the hydrocarbon curve (e.g. HC-30).

This project has received funding from the European Union's Horizon 2020 research and innovation programme under grant agreement No 814975

Document data

Document Title:	D11.1 – Development, theoretical evaluation and preliminary assessment of requirements for horizontal division of ro-ro spaces		
Work Package:	WP11 – Containment		
Related Task(s):	T11.2, T11.3		
Dissemination level:	Public		
Deliverable type:	R, Report		
Lead beneficiary:	01 – RISE		
Responsible author:	Pierrick Mindykowski		
Co-authors:	Maria Hjohlman, Robert Svensson		
Date of delivery:	March 2, 2022		
References:	D11.1, D09.2		
Approved by	Pascal Boulet on [2022-02-25]	Martin Carlsson on [2022-02-25]	Franz Evegren on [2022-03-02]

Involved partners

No.	Short name	Full name of Partner	Name and contact info of persons involved
01	RISE	Research Institutes of Sweden AB	Pierrick Mindykowski, Pierrick.mindykowski@ri.se Maria Hjohlman, maria.hjohlman@ri.se Robert Svensson, robert.svensson@ri.se
09	BV	Bureau Veritas Marine & Offshore Registre International De Classification De Navires Et De Plateformes Offshore	Blandine Vicard, blandine.vicard@bureauveritas.com Jerome Leroux

Document history

Version	Date	Prepared by	Description
01	2020-04-24	Pierrick Mindykowski	Draft of structure
02	2021-07-14	Pierrick Mindykowski	Circulated to reviewers
03	2022-02-14	Maria Hjohlman Robert Svensson	Updated with revision of Section 6-9. Circulated to reviewers
04	2022-02-25	Pierrick Mindykowski	Final version

Content

1 Executive summary

Main author of the chapter: Pierrick Mindykowski, RISE.

1.1 Problem definition

Concerning the fire integrity of the boundaries of ro-ro spaces, SOLAS requires A-60 thermal insulation for ships carrying more than 36 passengers, and A-30 between two ro-ro space) for ship carrying no more than 36 passengers.

The International Maritime Organization, through its correspondence group on fire safety, has underlined the need for more scientific studies regarding the performance of A-60 fire integrity of ro-ro spaces in case of fire.

1.2 Technical approach

To obtain a possible heat exposure from a realistic fire which can be encountered in a ro-ro space, results from tunnel fire tests were analysed and simulations were performed using Computational Fluid Dynamics. For the simulations, two representative ro-ro spaces were defined: a closed and an open ro-ro space, based on the existing ship STENA Flavia. Concerning the cargo, the ro-ro spaces were assumed fully loaded with trucks. The main results of the analysis are the highest temperatures monitored during a realistic fire in a ro-ro space and the size of the areas exposed to those temperatures. The temperatures were compared with time-temperature curves used in fire resistance testing and approval of thermal insulation.

Experimental tests consisting of exposing type approved thermal insulation to a more realistic time-temperature curve were carried out to assess the performance of relevant thermal insulations. Different thermal insulations (stone wool and glass wool-based insulation) were tested with various steel plate thicknesses, representing different uses of the ro-ro space (5 mm steel plate as per standard tests, 6 mm steel plate for ro-ro spaces dedicated to car storage, 12 mm steel plate for ro-ro spaces dedicated to truck storage).

1.3 Results and achievements

The main result from the simulations was that the heat exposure from a realistic fire in a ro-ro space is better represented by the hydrocarbon time-temperature curve, which is more severe than the standard (cellulosic) time-temperature curve used for test and approval of thermal insulation according to the FTP Code. However, one exception was found for completely closed ro-ro spaces (i.e. no openings at all) and with the ventilation turned off, a scenario where the fire was supressed due to oxygen depletion.

Experimental tests showed a significantly reduced fire integrity of approved thermal insulation when exposed to the hydrocarbon time-temperature curve. The reduction of the protection time was about 50% depending on the thickness of the steel plate for thermal insulation based on stone wool. Glass wool thermal insulation was deteriorated when exposed to the hydrocarbon time-temperature curve.

It is clear that the addition of thermal insulation between decks within the same horizontal fire zone increases the fire safety of ships. The present study goes even further by demonstrating that the current type of approved thermal insulation presents a reduced time of fire protection compared to expected protection time.

1.4 Contribution to LASH FIRE objectives

The work presented in this report contributes to the objectives of WP11, Action 11-A, to eliminate significant containment weaknesses, considering smoke, fire and heat integrity, by exploring new means for fire integrity sub-division of ro-ro spaces.

1.5 Exploitation and implementation

The results of this study will increase the awareness of the maritime community about the real protection time of certified thermal insulation. A reduction of 50% of the fire protection time should be considered when using stone wool based thermal insulation. More importantly, significant care should be taken when using glass wool based thermal insulation as it shows a poor ability to maintain fire protection capacity when exposed to severe heat exposure.

2 List of symbols and abbreviations

ACPH	Air changes per hour
CFD	Computational Fluid Dynamics
FDS	Fire Dynamics Simulator
FTP	Fire Test Procedures
HC	Hydrocarbon
HGV	Heavy Goods Vehicle
HRR	Heat Release Rate
HRRPUA	Heat Release Rate Per Unit Area
IACS	International Association of Classification Societies
IMO	International Maritime Organization
MSC	Maritime Safety Committee
MVZ	Main Vertical Zone
RISE	Research Institutes of Sweden
SOLAS	Safety Of Life At Sea
TC	Thermocouple

3 Introduction

Main author of the chapter: Pierrick Mindykowski, RISE

Ro-ro ships have been an important component of the commercial maritime industry since their introduction in the 1940's. The ships have a large longitudinal space where cars, trucks and other cargo can be rolled on and rolled off. Despite improved fire protection regulations, many fire accidents have occurred on ro-ro ships and there are no signs of them diminishing in number or magnitude. This was a conclusion at the IMO [1] based on a statistical study of ship fires, which has led to an ongoing update of the international fire safety regulations for ro-ro ships in SOLAS Chapter II-2 [2] and associated codes. During a review of the fire safety regulations [1], the IMO correspondence group has particularly pinpointed the need for additional experimental data or results of scientific studies regarding:

- The performance of A-60 boundaries in case of a ro-ro space fire, especially to prevent fire spread to accommodation spaces; and
- The performance of A-0 boundaries in case of a ro-ro space fire, especially to prevent fire spread between ro-ro spaces.

The purpose of the present study was to clarify the performance of state-of-the-art fire integrity between decks within the same ro-ro space and to give recommendations about on how sufficient fire containment is ensured.

The present report starts by presenting a regulations study concerning horizontal division of ro-ro spaces. This literature study reviews applicable regulations and aims to explain the fire integrity requirements for the boundaries of ro-ro spaces.

Considering those requirements, the in the aim of this report was to establish safe design regarding thermal insulation within ro-ro spaces. This was achieved by first determining the possible ceiling heat exposure from a realistic fire within representative ro-ro spaces (open and closed ro-ro spaces) fully loaded with trucks. Results from fire tests conducted for similar scenarios, i.e. tunnel fire tests, were analysed. These results were complemented with computational fluid dynamic (CFD) simulations using Fire Dynamics Simulators (FDS) to monitor the temperatures reached at the ceiling. These temperatures were then compared with time-temperature curves used in fire safety engineering and approval of thermal insulation. From this comparison, the best fitting time-temperature curve was selected and then used in experimental tests with a reduced scale furnace. These tests were carried out to compare the actual performance of approved thermal insulation when exposed to what was considered to be a realistic worst-case heat exposure in a ro-ro space.

4 Regulation review concerning horizontal division of ro-ro spaces

Main authors of the chapter: Blandine Vicard (BV), Jérome Leroux (BV)

4.1 General

4.1.1 Applicable regulations

The present review is based on the currently applicable regulations. Therefore, some of the requirements detailed below may not be applicable on old ships.

A brief summary of the main regulation changes is provided in Table 1.

Table 1. Summary of regulation changes

Regulation change	Application date	Adoption date	Summary
SOLAS 74	1980[1]	1974	Introduces the principle of horizontal fire zone for ro-ro spaces / special category spaces with: • Structural fire protection • Fixed fire extinguishing system ("drencher" type) • Fixed fire detection system
MSC.338(91)	01/07/2014	30/11/2012	Raises the fire integrity requirements for ro-ro and vehicle spaces onboard cargo and passenger ships carrying not more than 36 passengers

The review was mainly based on the documents listed in Table 2.

[1] It is to be noted that the concept of horizontal fire zone and associated safety measures has actually been introduced in SOLAS 60 part H as per IMO resolution A.122(V) dated October 1967. However, the circular was never made mandatory and Part H was therefore only applied on a voluntary basis until SOLAS 74 came into force. Compliance with Part H is formally recognized to be equivalent with SOLAS 74.

Table 2. List of documents used for the review of regulations.

IMO Documents	SOLAS Convention, as amended
	2010 FTP Code, as amended
	MSC.1/Circ.1120, Unified Interpretations of SOLAS Chapter II-2, The FSS Code, The FTP Code and related Fire Test Procedures
	MSC.1/Circ.1615, Interim Guidelines for minimizing the incidence and consequences of fires in ro-ro spaces and special category spaces of new and existing ro-ro passenger ships
IACS & Class Rules	IACS Blue book dated January 2019
	BV Rules for Steel Ships (NR467), as amended in July 2019
	DNVGL Rules for the Classification of Ships, January 2017
	LR Rules and Regulations for the Classification of Ships, July 2016
Flag Administration Rules	MMF (French Flag Administration) Division 221 "Passenger ships engaged in international voyages and cargo ships of more than 500 gross tonnage", 28/12/17 edition
	US Coast Guard Code of Federal Regulations (CFR) 46, 2019 online edition
	Swedish Transport Agency "Comments and interpretations by the Swedish Transport Agency regarding IMO Conventions", version 03 dd.15/05/2017
	MCA (UK Flag Administration) Guidance on SOLAS Ch.II-2

4.1.2 Definitions

This section provides the definitions of key terms used in regulations relevant to fire integrity sub-division and horizontal divisions of ro-ro spaces.

4.1.2.1 Ro-ro space, vehicle space and special category space

As per SOLAS II-2/3:

- *"Vehicle spaces are cargo spaces intended for carriage of motor vehicles with fuel in their tanks for their own propulsion."*
- *"Ro-ro spaces are spaces not normally subdivided in any way and normally extending to either a substantial length or the entire length of the ship in which motor vehicles with fuel in their tanks for their own propulsion and/or goods (packaged or in bulk, in or on rail or road cars, vehicles (including road or rail tankers), trailers, containers, pallets, demountable tanks or in or on similar stowage units or other receptacles) can be loaded and unloaded normally in a horizontal direction."*[2]
- *"Special category spaces are those enclosed vehicle spaces above and below the bulkhead deck, into and from which vehicles can be driven and to which passengers have access. Special category spaces may be accommodated on more than one deck provided that the total overall clear height for vehicles does not exceed 10 m."*

  Special category spaces are ro-ro spaces to which passengers have access, possibly during the voyage. Special category spaces are the most frequent type of closed ro-ro spaces on ro-ro passenger ships.

  It is to be noted that open ro-ro spaces are not considered as special category spaces.

[2] In other words, ro-ro spaces are vehicle spaces into which vehicles can be driven. It is to be noted however that, for the purpose of the application of SOLAS II-2/19, the following interpretation can be found in MSC.1/Circ.1120 and IACS UI SC 85: "Ro-ro spaces include special category spaces and vehicle spaces"

4.1.2.2 Closed, open and weather deck

As per SOLAS II-2/3:

- A "*weather deck is a deck which is completely exposed to the weather from above and from at least two sides.*"
  IACS UI SC 86 additionally details that: "For the purposes of Reg. II-2/19 a ro-ro space fully open above and with full openings in both ends may be treated as a weather deck."
  For practical purposes, drencher fire-extinguishing system cannot be fitted on weather decks due to the absence of deckhead. This criterion is often used for a practical definition of weather decks.
- An open vehicle or ro-ro space is "*either open at both ends or [has] an opening at one end and [is] provided with adequate natural ventilation effective over [its] entire length through permanent openings distributed in the side plating or deckhead or from above, having a total area of at least 10% of the total area of the space sides.*"
- A closed vehicle or ro-ro space is any vehicle or ro-ro space which is neither open nor a weather deck.
  As a reference criterion, it can be considered that a vehicle space that needs mechanical ventilation is a closed vehicle space.

4.2 Requirements

4.2.1 General

This section describes the general requirements related to containment and provides the associated reference(s) in the regulatory texts.

SOLAS II-2/9 details a very comprehensive set of measures for the purpose of containing a fire onboard a ship. The approach relies on a categorisation of each space, taking into account as a background both the fire risk in the space and the criticality of losing it. Basically:

- Some spaces are identified as key elements to ensure either proper fire-fighting or evacuation. Those are basically the control stations and the escape routes. Those spaces are to be preserved as much as possible from any fire.
- Other spaces are regarded as potential fire risks (with various risk levels) and the aim is to prevent a fire from spreading from and to those spaces.

Then SOLAS includes specific fire containment requirements including summary tables detailing the required level of fire integrity between spaces for the following ship categories:

- Passenger ships carrying more than 36 passengers;
- Passenger ships carrying not more than 36 passengers;
- Cargo ships other than tankers; and
- Tankers.

[SOLAS II-2/9]

Ro-ro spaces can be found on the first three types of ships. The corresponding fire containment requirements are detailed below.

4.2.2 Horizontal fire zones on passenger ships

[SOLAS II-2/2.2]

In principle, passenger ships are separated into main vertical zones, the length of which is normally limited to 40 meters[3]. In order to accommodate garage spaces spanning potentially over the whole length of the ship, SOLAS II-2/20.2.2 allows the definition of horizontal zones which "*may include special category spaces on more than one deck provided that the total overall clear height for vehicles does not exceed 10 meters*[4]". The required integrity for horizontal fire zones is the same as for main fire zones i.e.:

- A-60 fire integrity on passenger ships carrying more than 36 passengers, which may be reduced to A-0 where the space on the other side of the fire division has a very low fire risk (open decks, sanitary spaces or tanks, voids and machinery spaces with little or no fire risk)
- A class fire integrity on passenger ships carrying not more than 36 passengers, with detailed ratings in line with Table 3.

"Main vertical zone boundary integrity" also refers to complementary requirements, especially regarding the doors leading to the ro-ro vehicle spaces including, for practical purposes, that:

- Those doors are to be self-closing
- An indication that they are properly closed is to be available in the continuously manned central control station
- Arrangements are to be made to ensure local control of the doors, including power-operated doors, also taking into account the case of a fire (door to be operable up to 200°C)

[SOLAS II-2/9.4.1.1.5]

It should also be noted that the concept of the horizontal fire zone is also associated with an efficient fire-extinguishing system.

4.2.3 Fire integrity requirements for the boundaries of ro-ro and vehicle spaces

[SOLAS II-2/9.6.1]

On passenger ships carrying more than 36 passengers, the boundaries–decks and bulkheads–of ro-ro and special category spaces are required to have A-60 fire integrity. This fire integrity level may however be reduced to A-0 where the space on the other side of the fire division has a very low fire risk (open decks, sanitary spaces or tanks, voids and machinery spaces with little or no fire risk).

[SOLAS II-2/20.5]

The fire integrity level required between ro-ro or vehicle spaces and other space on cargo ships and passenger ships carrying not more than 36 passengers is summarized in Table 3 below.

[SOLAS II-2/9 Tables 9.3, 9.4, 9.5 and 9.6]

[3] The length and width of main vertical zones may be extended to a maximum of 48 m (MVZ bulkheads to coincide with watertight bulkheads) or total area of MVZ must not be greater than 1600 m2 on any deck (to accommodate large public spaces, for instance)

[4] The way to measure this 10m height is further clarified in IMO MSC.1/Circ.1120 and IACS UI SC158.

Table 3. Fire integrity requirements around ro-ro or vehicle spaces on cargo ships and passenger ships carrying not more than 36 passengers

	Space categories	Fire integrity requirement with respect to a ro-ro or vehicle space
Key spaces to be preserved	Control stations	A-60
	Stairways and corridors	A-30
Potential fire risks	Category A machinery spaces	A-60
	Accommodation spaces and high fire risk service spaces	A-30
	Low risk service spaces, machinery spaces other than category A machinery spaces, open decks	A-0
	Cargo spaces (other than ro-ro and vehicle spaces)	A-0
	Other ro-ro or vehicle spaces	A-30

For practical purposes, there is no fire integrity requirement around a weather deck intended to carry vehicles, only a steel bulkhead or deck is required between such an area and another enclosed space.

The Swedish Flag nevertheless clarifies that, on cargo ships, weather decks intended to carry vehicles are to be considered as the same category as enclosed ro-ro or vehicle spaces, and therefore similarly insulated with respect to other spaces.

[Comments and interpretations by the Swedish Transport Agency regarding IMO Conventions, interpretation of SOLAS II-2/9.2.3.3.2.2 (11)]

It is to be noted that the fire integrity requirements for ro-ro and vehicle spaces have been reinforced by MSC.338(91) amending SOLAS requirements for ships constructed after 01/07/2014. Prior to this date:

- There was no firm fire integrity requirement between two ro-ro or vehicle spaces, only this footnote "*Bulkheads and decks separating ro-ro spaces shall be capable of being closed reasonably gastight and such divisions shall have "A" class integrity in so far as reasonable and practicable, if in the opinion of the Administration it has little or no fire risk.*"
- There was no fire integrity requirement between an open deck and a ro-ro or vehicle space, a mere steel bulkhead or deck was acceptable.

4.2.4 Fire integrity

Fire integrity as per SOLAS corresponds to fire testing standards defined in IMO FTP Code. Dedicated fire test procedures are available for:

- Decks and bulkheads
- Pipe, duct and electrical cable penetrations
- Doors and windows
- Fire dampers

SOLAS II-2/3 provides the following definition:

> *"A" class divisions" are those divisions formed by bulkheads and decks which comply with the following criteria:*

1. *they are constructed of steel or other equivalent material;*
2. *they are suitably stiffened;*
3. *they are insulated with approved non-combustible materials such that the average temperature of the unexposed side will not rise more than 140°C above the original temperature, nor will the temperature, at any one point, including any joint, rise more than 180°C above the original temperature, within the time listed below:*

class "A-60"	*60 min*
class "A-30"	*30 min*
class "A-15"	*15 min*
class "A-0"	*0 min*

4. *they are constructed as to be capable of preventing the passage of smoke and flame to the end of the one-hour standard fire test; and*
5. *the Administration has required a test of a prototype bulkhead or deck in accordance with the Fire Test Procedures Code to ensure that it meets the above requirements for integrity and temperature rise.*

5 Need for better requirements concerning the horizontal division of ro-ro spaces

Main authors of the chapter: Pierrick Mindykowski (RISE)

RISE has investigated the potential for fire spread through internal decks sub-dividing a ro-ro space, as described for special category spaces in paragraph 4.2.2 [3]. Indeed, when a ro-ro space is sub-divided, only steel or A-0 may be used. This kind of protection might imply a risk of fire propagation from the lower part of the space to the upper one. This risk has been quantified by RISE through experiments. A series of tests was performed regarding the fire growth and vertical fire spread through a steel deck with lashing holes. The test set up simulated a burning car by a gas burner exposing a steel deck (6m by 1.6 m) above and evaluated fire spread.

The fire growth was measured with a calorimeter and the vertical fire spread was determined by temperature measurements in relevant positions and by monitoring the time to ignition of targets simulating tires and lashing ropes at the unexposed side of the test specimen. The main result of those tests was that a tyre is ignited, when positioned close to a lashing hole, after 10 minutes, mainly due to hot gases.

Moreover, in 2010 China, during the 54th session of the IMO Fire Protection subcommittee, submitted a proposal to the International Maritime Organization regarding amendments to the requirements of fire integrity for boundary bulkheads and decks of ro-ro spaces of passenger ships carrying no more than 36 passengers and cargo ships. In this document, China referred to the investigation report of the fire accident of the ro-ro cargo ship Und Adriyatik. Indeed, it shows that the fire spread to several decks within 10-15 minutes due to the absence of fire integrity of the ro-ro space boundaries. This result may be compared to the previously described RISE experiment as well as the following SP study [3] that included tests and calculations showing that a fire that occurs in a ro-ro space of a cargo ship can grow to almost 80 MW and reach an average gas temperature between 250 and 300°C.

The previous studies have demonstrated the need for a higher requirement concerning the horizontal division of ro-ro spaces, as well as further studies considering the development and consequences of a realistic heat exposure on thermal insulation in a ro-ro space.

6 Methods used to determine realistic fire exposure

Main authors of the chapter: Maria Hjohlman (RISE)

In order to define a realistic heat exposure, fire tests representing fire scenarios similar to what can be expected in an open ro-ro space were studied. For a fire in an open ro-ro space, tunnel fire tests were found to be a valuable source of information.

These real fire tests were complemented with numerical simulations of fires in both open and closed ro-ro spaces that were considered as realistic based on real cargo representations. The software used is Fire Dynamics Simulator (FDS). It is a computational fluid dynamics (CFD) model of fire-driven flow. For a detailed description, please revert to the user guide of FDS [4]. Selected for the study as representative cargo were heavy goods vehicles (HGV).

As described in paragraph 4.2.4, the standard time-temperature curve used for the approval of thermal insulation (for ships as well as buildings) is the ISO 834 curve. This curve has been developed to represent the typical temperatures encountered in a building, based on a cellulosic-based fire. Due to the high temperatures found in the present study, another time-temperature curve was of interest, namely the hydrocarbon-based fire load curve (HC curve), commonly used in offshore applications. The two time-temperature curves are presented in Figure 1.

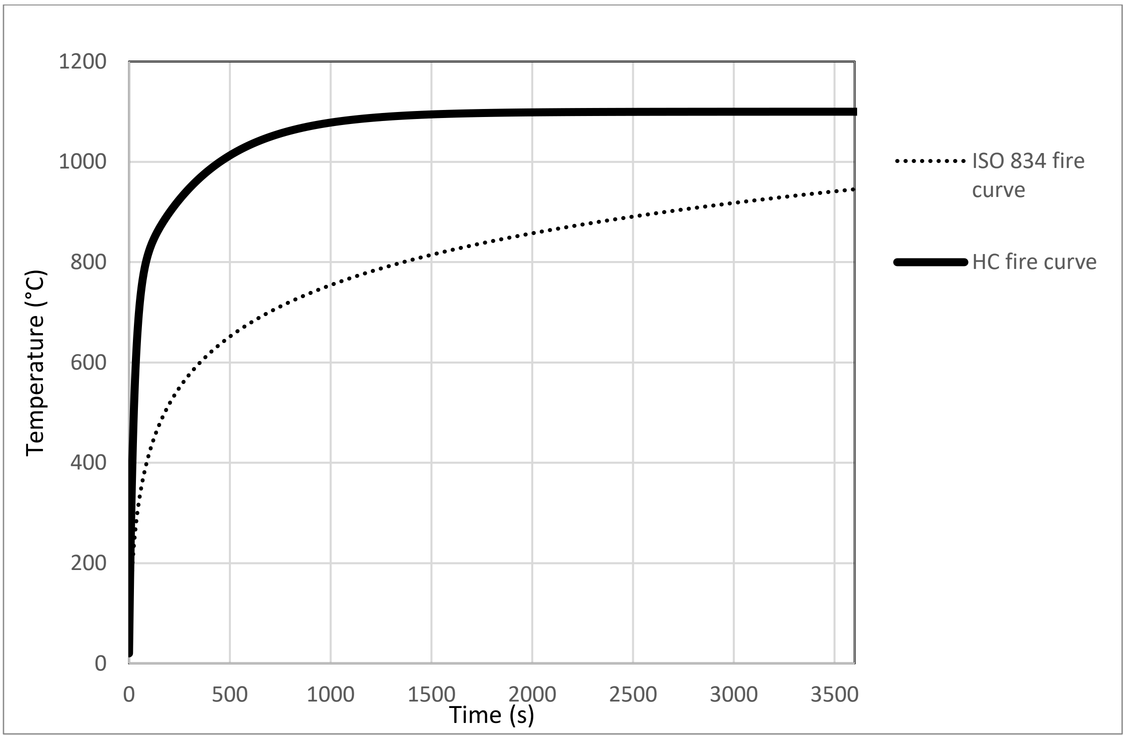

Figure 1. Illustration of the ISO 834 and hydrocarbon time-temperature curves.

As expected by the nature of the combustible, the HC curve poses a more severe heat exposure than the ISO 834 curve. The realistic heat exposures found from the fire tests and obtained in the simulations will below be presented together with the ISO 834 and the hydrocarbon time-temperature curves, for comparison reasons.

It should be noted that the ro-ro spaces in a ro-ro passenger ship are equipped with drencher systems. When functioning properly, the systems are expected to control the fire and consequently, the heat release rates (HRR) and temperatures presented in this study would not occur. This study was conducted under the assumption the drencher system fails to start or for other reasons is not functioning properly in supressing the fire and cooling the smoke gases.

7 Review of fire tests involving HGV under similar conditions to fires in open ro-ro space

Main authors of the chapter: Maria Hjohlman (RISE)

A useful source for studying realistic ceiling gas temperatures during fires in HGVs are tunnel fire tests conducted over the last decades. These tests have been run under well-controlled and well-documented conditions and several tests involve an HGV, as a real vehicle or as a mock-up. The HGV (or the muck-up) carries goods, typical for this type of vehicle, consisting of wood, plastic material, carboard or a mixture thereof (e.g. furniture). Three tunnel fire test series were selected for the study and are presented in section 7.1. However, the relevance of temperature curves measured during tunnel fire tests could be questioned when discussing ro-ro space fire tests and they will be further discussed below. The differences in geometry and ventilation conditions are also of interest.

The ceiling heights in the fire tests are in the same order of magnitude as those found in ro-ro spaces (approximately 5-5.2 m compared to 5.8 – 6.0 m as specified for the generic ship Stena Flavia). The height of the HGVs in the fire tests are typical height for these types of vehicles. Adding the effect of the ceiling beams at the ro-ro space that, for Stena Flavia, extends down 0.8 – 1.0 m, the space between the truck load and the ceiling is considered to be similar.

The widths of the tunnels were in the range of 5.3 to 7.2 m. The walls could induce a higher re-radiation back to the burning truck with an increase in HRR as a result. On the other hand, this effect could be seen also from the surrounding trucks, the ceiling and, for the trucks parked close to the walls, i.e. the walls of the ro-ro space. Even if the two tunnel side walls form a different enclosure compared to a ro-ro space, it will be a scenario with more similarities to a burning truck surrounded by other trucks (and possibly one wall) in a ro-ro space than would be the case for a burning HGV in an open field.

Another effect of the geometry of the tunnel is that the flow of smoke gases is directed along the tunnel (as opposed to in a ro-ro space where it can travel in a more radial direction), which possibly causes less entrainment of air in the smoke gases, resulting in a lower volume and higher temperatures of the smoke gases. Comparing to a fire in an open ro-ro space where wind conditions cause a directed flow of air through the space and the trapping of smoke gases in the semi-compartments formed by the transversal and longitudinal ceiling beams, these differences are judged to be of minor importance.

In the tunnel fire tests a controlled flow of air through the tunnel is typically applied at the up-stream tunnel opening to make sure measurements of the smoke gases can be conducted at specific positions under a controlled direction of gas flow (avoiding so called back-layering where hot smoke under the ceiling travels up-stream). Experience has shown an air flow of around 3 m/s is sufficient, which is the reason for why this level of air flow is often seen in tunnel fire tests.

It is a well-known fact that ventilation of air often increases the HRR of a burning object. Numerical simulations of an open ro-ro space under typical side wind conditions showed an air flow in the range of 1.0-3.5 m/s for a majority of the ro-ro spaces and up to above 4.5 m/s close to the wind exposed openings (Figure 18). The high HRR levels found in the tunnel fire tests were therefore considered to be possible for this type of vehicles in an open ro-ro space.

7.1 Selected tunnel fire tests

7.1.1 EUREKA/EU499 FIRETUNE 1990-1992

A total of 21 fire tests were conducted in the Rappafjord tunnel, Norway, during 1990-1992 [5]. Test 21 involved an HGV loaded with a mixture of furniture made of wood, fabric, fibre boards, mattresses and upholstery, representing a typical combustible truck load. The driver's cab was equipped with a furnished sleeping area. The vehicle had a length of 16.1 m and the total calorific value for the load and vehicle was estimated to 87.4 GJ.

The tunnel was 2.3 km long with a width of 5.3-7.0 m and a height of 5 m at the location of the fire source. The longitudinal ventilation was controlled by a fan at the upstream tunnel opening. The ventilation rate through the tunnel was varying to see the effect on the fire. Initially the air flow was approximately 6 m/s during the first 13.5 minutes of the test, then no forced ventilation was applied for 3 minutes, followed by 2-3.8 m/s until the end of the test.

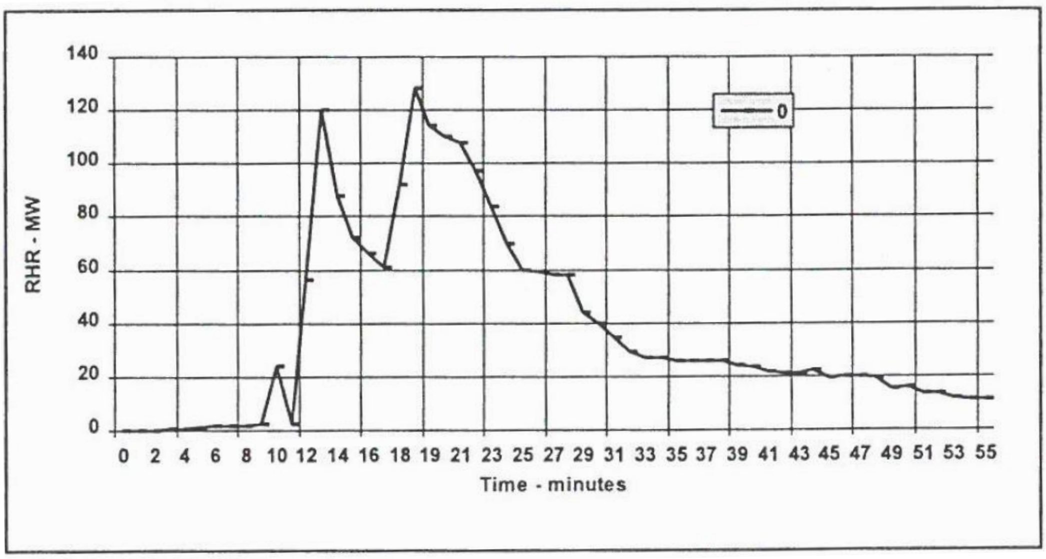

Figure 2. HRR estimated in the EUREKA/EU499 FIRETUNE fire test #21. [5]

7.1.2 Runehamar 2003

In the Runehamar tunnel, four fire tests were conducted with HGV mock-ups in 2003 [6]. The mock-up carried various goods in the four fire tests, as presented in Table 4.

Table 4. Fire sources in the Runehamar tunnel fire tests.

Test	Load on HGV muck-up	Theoretical calorific energy (GJ)
T1	A mixture of wood and plastic pallets (380 wood pallets and 74 PE plastic pallets).	244
T2	216 wood pallets and 240 PUR mattresses.	135
T3	Furniture and fixtures (tightly packed wood and plastic cabinet doors mixed with upholstered furniture, stuffed toy animals, wood and plastic toys, etc), 10 large rubber tyres.	179
T4	600 corrugated paper cartons with PS plastic cups on 40 wood pallets.	62

All goods were arranged on a steel platform at the height of 1.1 m in a storage steel rack frame. The total arrangement measured 10.4 m long, 2.9 m wide and 4.5 m high and was covered by a polyester tarpaulin.

The Runehamar tunnel is approximately 1 600 m long and the cross section at the fire site was 7.1 m wide and 5 m high. At the upstream tunnel opening a mobile fan generated a longitudinal ventilation in the range of 2.8 – 3 m/s. This flow decreased during the fire tests down to approximately 2.4-2.5 m/s due to flow resistance of the fire and thermal stack effects.

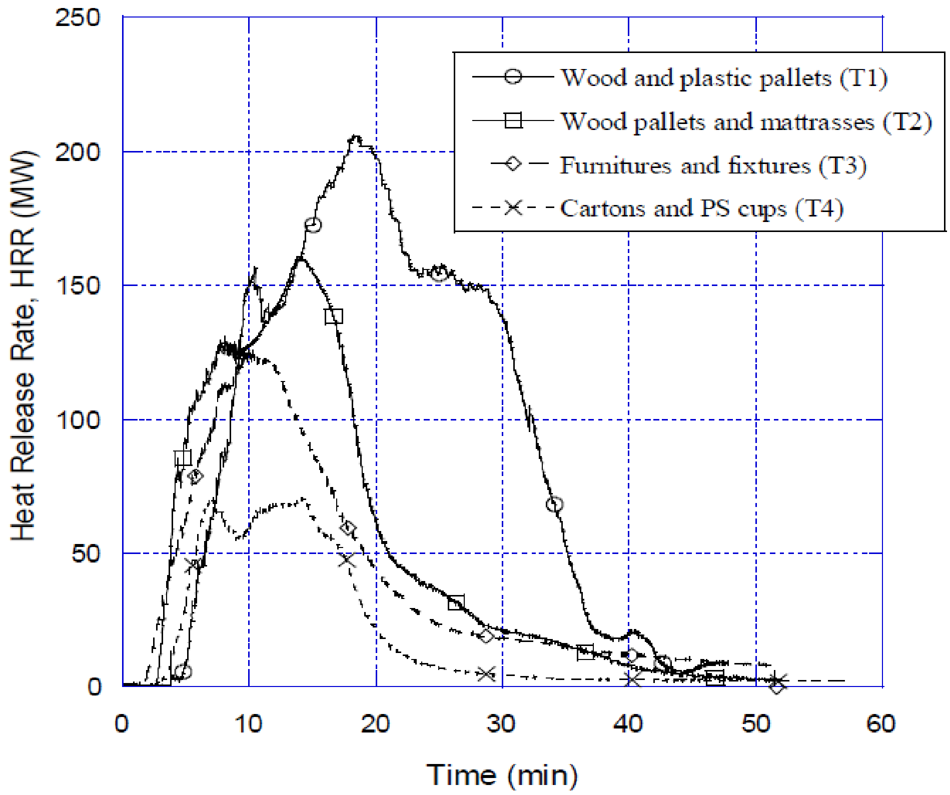

The estimated HRR produced in the fire tests for each of the four tests are presented in Figure 3.

Figure 3. HRR from HGV mock-ups estimated at the Runehamar 2003 fire tests. [6]

7.1.3 Cheong et al. 2012

A series of large-scale fire tests with simulated heavy goods vehicles (HGV) was conducted in a test tunnel facility in Spain [7]. The fire source was an HGV mock-up loaded with 48 plastic pallets (20%) and 180 wooden pallets (80%), for a total of 228 pallets. The pallets were arranged on a 1 m high platform, surrounded by a steel frame with a top steel plate. The total arrangement was covered by a plastic tarpaulin and measured 2 m wide, 7.5 m long, reaching 4 m above ground. Six of the seven tests were involving a sprinkler system, the seventh test was conducted as a free burn test without the sprinkler system (Test 7).

The tunnel was a two-lane 600 m long road tunnel. The section at the location of the fire measured 5.2 m in height and 7.2 m in width. Jet fans at the upstream opening of the tunnel generated an air flow of 3 m/s for the entire duration of the fire test. The heat release rate (HRR) generated are presented in Figure 4.

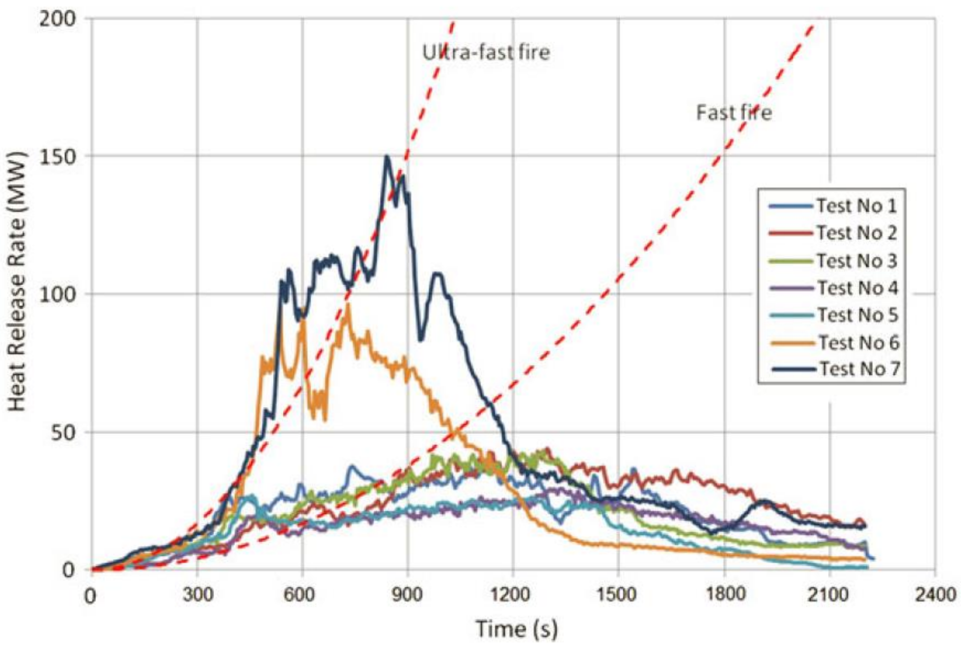

Figure 4. Estimated HRR generated in the tests. Test 7 was the free-burn test, while the other tests involved sprinklers. [7]

7.2 Summary of hot gas heat exposure on ceiling obtained at tunnel fire tests

In all six fire tests the gas temperatures close to the ceiling at the longitudinal centre of the tunnels were measured. Temperatures measured above the HGV from the different tests were compiled in one graph in Figure 5. Temperatures from the tests by Cheong and Eureka tests were manually digitized from the literature, while the curves of the Runehamar tests were based on the original source data (presented as a 20 s running average). It should be noted the curves were shifted to synchronise the onset of temperature rise to 0 s, hence, the time scale is not in correlation with the previously presented HRR curves.

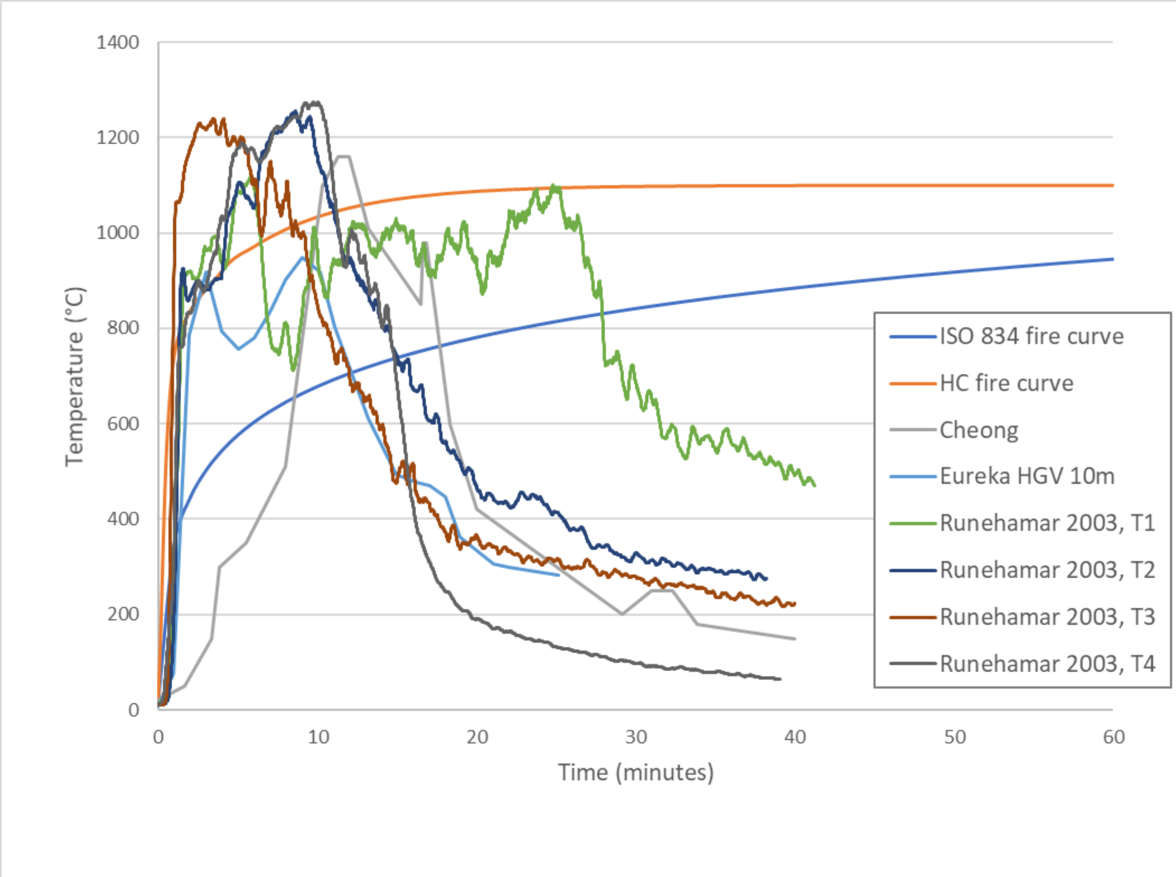

Figure 5. Temperatures under the ceiling close to burning HGVs (mock-up or real). Onset of temperatures were shifted to time=0 and do not correlate to previously presented HRR curves. Temperatures are compared to the ISO 834 and HC time-temperature curves. Note, only one HGV was involved in each test; no fire spread to other vehicles was possible.

As is seen in Figure 5, the temperatures under the ceiling during the tunnel fire tests are considerably higher than the ISO 834 curve. In all tests, the temperatures temporarily (approximately 2 to 10 minutes) reach even above the HC curve.

As described above, only one HGV (or HGV mock-up) was present and the duration of the temperature curves are limited by the amount of material in a single HGV. With fires of those sizes, as indicated by the HRR and smoke gas temperatures, fires will most probably spread to an adjacent HGV when parked as close as is typically seen in a ro-ro space. Most likely, fires would spread from one vehicle to the next and has the potential to continue for hours until the combustible materials are consumed, only limited by the access of oxygen or a fire suppression system. In case of a ventilation-controlled fire, the HRR and temperature curves would have a considerably longer duration than presented here.

The temperatures presented in Figure 5 are point measurements and do not say anything about the size of the ceiling area being exposed to the heat, if it is only a small part right above the fire or if the flames and hot gases reach over a considerably larger area. If the area is large, the hot gas exposure to a point of the ceiling has the potential to be present for a longer duration when the fire spreads from one truck to another. To give an indication of the affected area, ceiling gas temperatures at locations downstream of the burning HGV from the Runehamar tests are presented in Figure 6. It is apparent that the temperatures close to the burning object reach similar temperatures of around 1200 °C in all tests, while the duration of the high temperatures relate to the duration of the HRR curve. A clear tendency is seen in that the higher HRR level obtained in the test, the longer the flames and hot gases reached downstream the tunnel. For HRR above and around 150 MW (T1 and T2), gas temperatures of 1000-1200 °C are seen at a distance as long as 40 m down the tunnel.

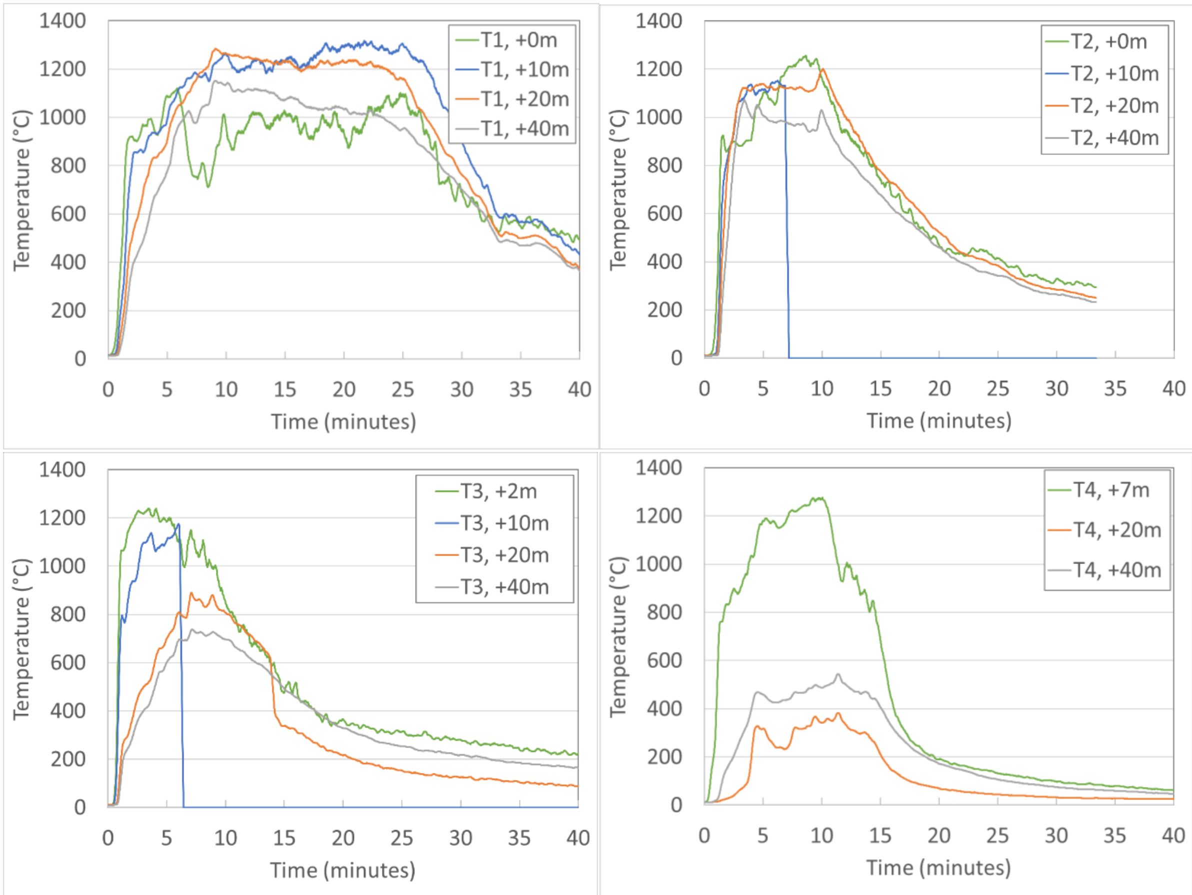

Figure 6. Longitudinal spread of hot gases in the Runehamar 2003 tests. Gas temperatures measured at tunnel centre close to ceiling downstream from the fire source at the indicated distance.

8 Numerical simulations of fires in open and closed ro-ro space

Main author of the chapter: Robert Svensson, RISE.

To investigate the gas temperatures close to the ceiling during a fire in a ro-ro space involving an HGV, the software Fire Dynamics Simulator (FDS) [4] has been used.

8.1 Scenario description

A total of four scenarios were investigated based on the results of the project RO5 [8], where it was demonstrated that an open ro-ro space gives a more severe fire due to the contribution of oxygen from side and end openings. The scenarios simulated are summarized in Table 5 and included one closed and one open ro-ro space, both with high and low ventilation conditions. For the closed ro-ro space, this implies either having a fully closed volume where all fans are off or having a total of 10 air changes per hour (ACPH). The open ro-ro space was simulated with no wind or with a side wind of 7.5 m/s. The duration for all simulations was set to 30 min. The fire source was the same in all simulations, with a max HRR of 120 MW.

Table 5: Simulated scenarios

Deck	Fire	Ventilation
Closed	Max HRR 120 MW	Closed
Closed	Max HRR 120 MW	10 ACPH
Open	Max HRR 120 MW	No wind
Open	Max HRR 120 MW	7.5 m/s side wind

8.2 Representation of realistic cargo in simulated ro-ro spaces

The representation of realistic cargo in the ro-ro spaces was based on an existing ship, STENA Flavia. The ro-ro spaces modelled in the present study were based on deck 3 and deck 4 of STENA Flavia, with the help of the following documents provided by Stena Rederi AB:

- General Arrangement
- Fire Control Plan
- Open ro-ro space General Arrangement
- Vehicle Deck Ventilation

Figure 7 presents the general arrangement of deck 3 and deck 4.

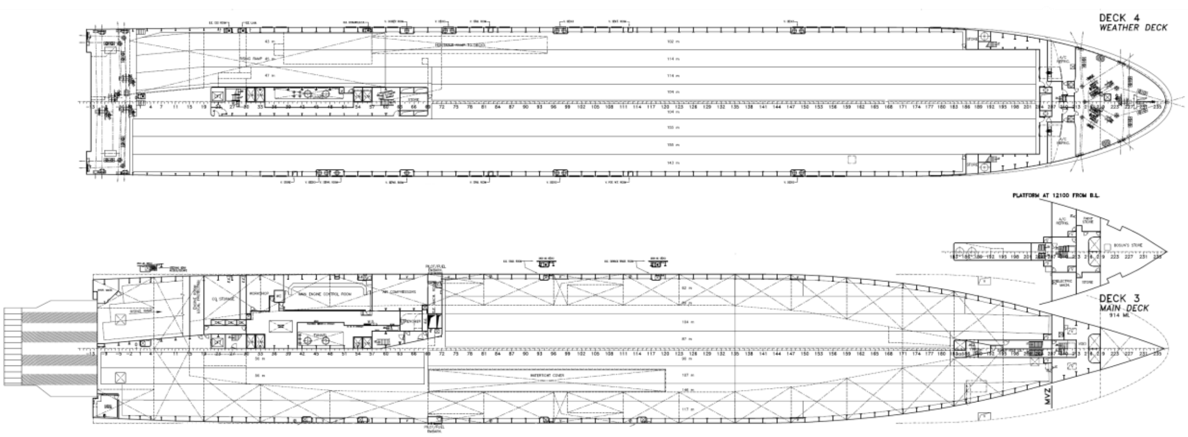

Figure 7. Deck 3 (lower) and 4 (upper) of the Stena Flavia.

8.3 Model geometries

It was decided for the present study to use two types of ro-ro spaces, a closed ro-ro space with no openings, and an open ro-ro space, based on decks 3 and 4 of STENA Flavia respectively.

The closed ro-ro space had the following inner dimensions:

- 162 m long
- 25.6 m wide
- 5.8 m high.

The model used in the simulations can be seen in Figure 8.

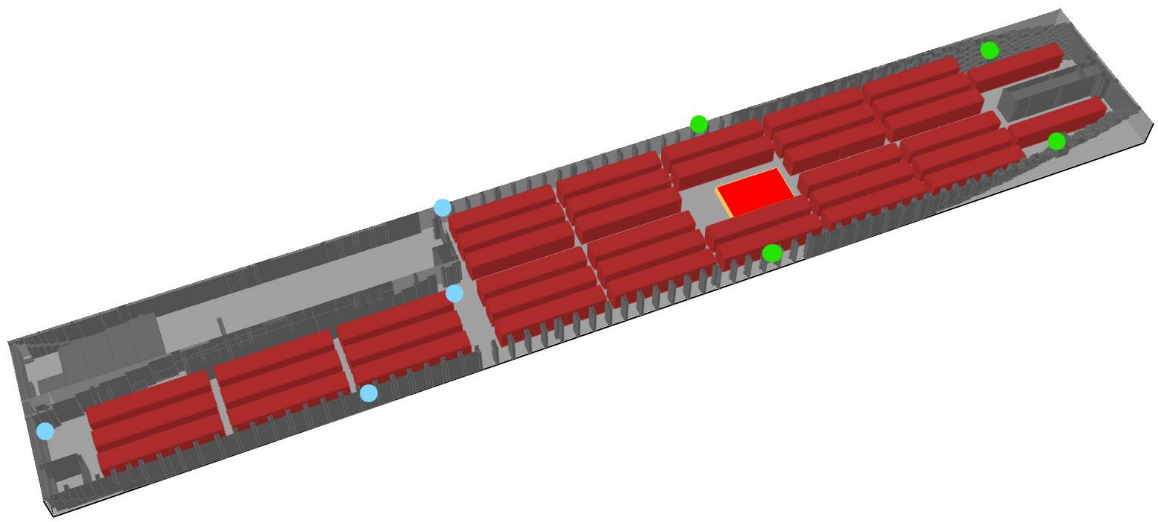

Figure 8: Closed ro-ro space based on STENA Flavia, deck 3. Green dots mark the positions of supply fans and blue dots mark the positions of the exhaust fans. The red area close to the middle is the fire source. The rectangular boxes represent trucks. The ceiling beam framework was represented but is hidden in the picture.

The open ro-ro space (deck 4) had the following inner dimensions:

- 156 m long
- 25.6 m wide
- 6 m high.

The models used for the simulations can be seen in Figure 9 and Figure 10.

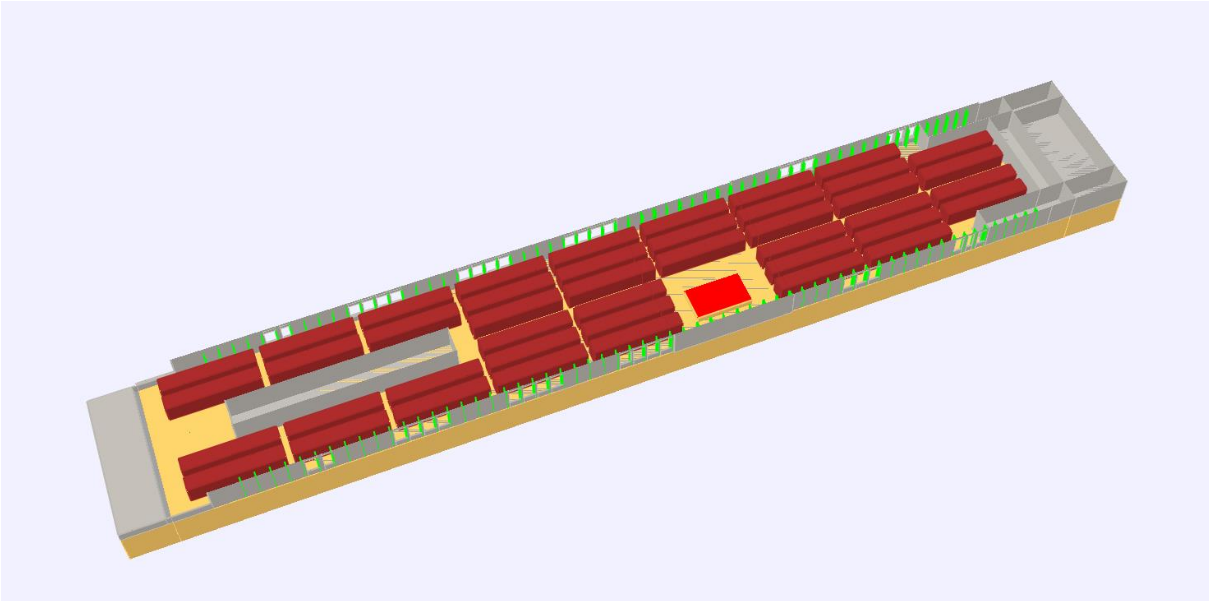

Figure 9: Open ro-ro space based on STENA Flavia deck 4. The red area close to the middle is the fire source. The rectangular boxes are representing trucks. The framework in the ceiling was represented but is hidden in the picture.

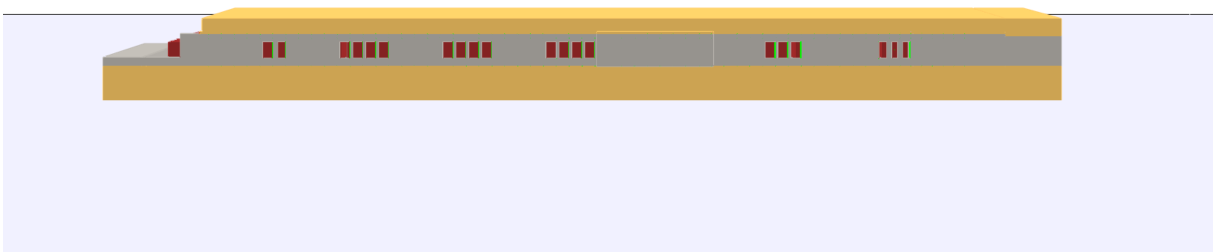

Figure 10: Sideview of the simulated closed ro-ro space. The outer geometry was simplified, and box like in comparison to the actual ship. The side openings of the ship can be seen in the picture.

8.3.1 Domain and discretization

The numerical grid of computational cells in FDS is rectilinear and constrains the geometry to follow this grid. Closest to the fire source and up to 10 m in all directions, the computational cells were 20 cm in all directions. Outside of this volume, the largest cells were 40 cm x 40 cm x 20 cm. For deck 4, the outdoor geometry was simulated with the largest cells furthest away from the ship measuring 3.2 m in all directions.

For the simulations of deck 4, the computational domain was extended to be 768 m x 377 m x 76.8 m in order to let the wind profile stabilize before reaching the ship.

The grid resolution is recommended to have a ratio of at least 10 < $D^*/\delta\mathrm{x}$ < 20 [4] where δx is the grid size and D^* is the characteristic fire diameter defined according to equation (1). The value will be above 10 for a fire larger than 6 MW and over 20 for a fire larger than 35 MW, which will be the case for the interesting period of the simulations.

$$D^* = \left(\frac{\dot{Q}}{\rho_\infty c_p T_\infty \sqrt{g}}\right)^{2/5} \quad (1)$$

where $\dot{Q}$ is the heat release rate [W], ρ_∞ is the ambient density of air [kg/m^3], $c_p$is the specific heat capacity of air [J/kg·K], T_∞ is the ambient temperature [K], and g is the gravitational acceleration [m/s^2].

8.3.2 Cargo

The cargo for the simulations was chosen to be trucks. The trucks were represented as rectangular boxes with the following dimensions: 15.6 m x 2.4 m x 3.2 m and are hovering 0.8 m above the floor. There is a 1 m space from the top of the boxes to the longitudinal and transversal beams at the ceiling. The boxes were made adiabatic, meaning that they have no energy exchange with their environment. There was placed a total of 39 trucks on deck 3 and 43 on deck 4. The volume of the trucks filled up 23 % and 24 % of the total volume of deck 3 and 4, respectively. The trucks were distributed to 6 lanes in comparison to the existing 8 lanes on the ship. The reason for the reduction in cargo density was to slightly widen the flue spaces between the trucks to avoid numerical instability.

8.3.3 Material properties

All surfaces constituting the ro-ro space were assumed to be steel with a thickness of 10 mm. Steel properties were taken from the Eurocode 3 [9] and are presented in Table 6.

Table 6: Steel properties according to Eurocode 3

Emissivity (-)	0.7
Density (kg/m^3)	7850
Specific heat (J/kg·K)	$450 + 0.28 \cdot T_s - 2.91 \cdot 10^{-4} \cdot T_s^2 + 1.34 \cdot 10^{-7} \cdot T_s^3$
Conductivity (W/m·K)	$14.6 + 1.27 \cdot 10^{-2} \cdot T_s$

T_s represents the temperature of the steel in Celsius.

The ceiling was insulated in the models of both decks to fulfil A-60 performance.

The A class division deck was modelled in accordance with the documents provided by STENA Rederi AB and consists of standard thermal insulation certified for A-60 performance.

Regarding the properties of the thermal insulation, they were taken from the manufacturers and are presented in Table 7.

Table 7: Thermal insulation properties

Material property		**A-60**
Thickness (cm)		7
Emissivity (-)		0.7
Density (kg/m^3)		56
Specific heat (kJ/kg·K)	T_i =100	0.84
	T_i =400	1.154
	T_i =600	1.212
	T_i =700	1.586
Conductivity (W/m·K)	T_i =10	0.031
	T_i =100	0.041

	T_i =200	0.057
	T_i =550	0.18
	T_i =650	0.22
	T_i =700	0.23

T_i represent the temperature of the thermal insulation in Celsius.

8.3.4 Ventilation for closed ro-ro space

For the closed ro-ro space, the model was a closed volume with eight pressure dependent fans: four supply fans in the front and four exhaust fans in the rear. The volume flow is dependent on the pressure difference between the ambient pressure outside the model and the pressure closest to the fan positions in the model, see Figure 11. At ambient pressure without a fire in the model, the total volume flow in the model was set to be 10 air changes per hour (ACPH) according to documents from STENA.

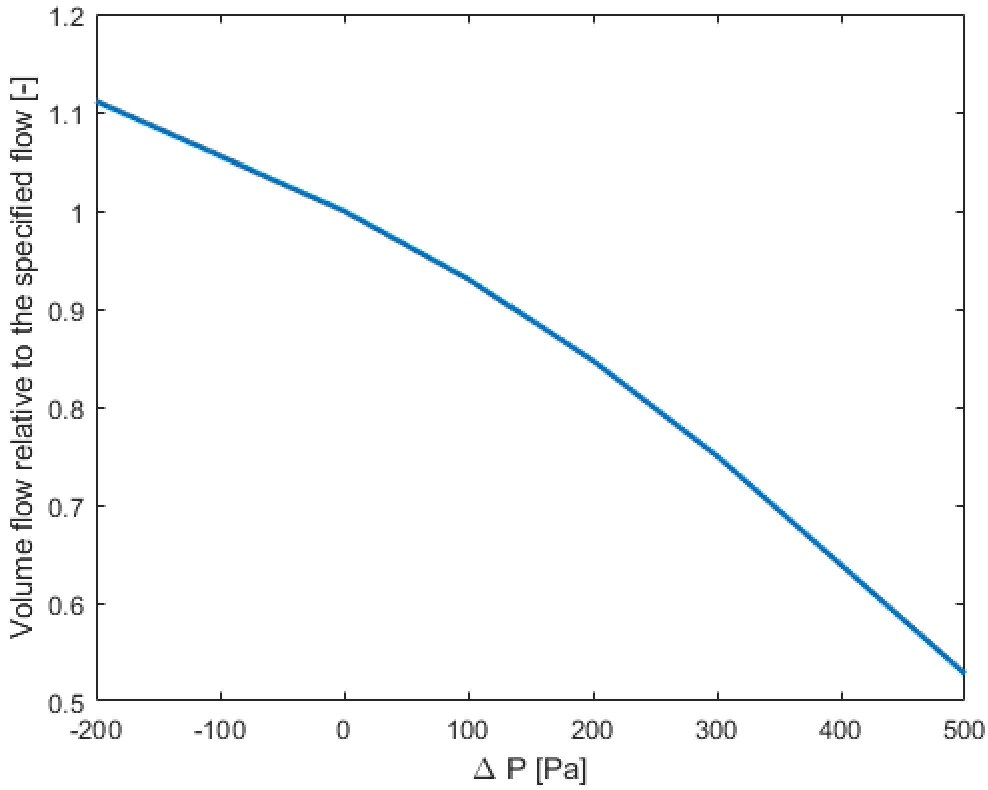

Figure 11: Fan curve used for simulations of closed ro-ro space. The expected aerodynamic resistance from the HVAC system was subtracted from the curve so the pressure difference is between the inside of ambient pressure outside the model and the pressure closest to the fan position in the model.

8.3.5 Ventilation for open ro-ro space

For the open ro-ro space, a model based on Stena Flavia deck 4 was used. The aft of the space was open to the outside. On the sides of the deck, several openings were modelled with the dimensions 1.9 m x 3.2 m, giving a total area equivalent to 13 % of the side area up to the furthest point of the loadable volume (clear height). The ventilation conditions were set as either having no wind at all or having a side wind perpendicular to the ship of 7.5 m/s, which is the average wind speed on the

Baltic Sea [10][11]. The wind profile depending on the height above the see level can be calculated according to:

$$u = u_0 \left(\frac{z}{z_0}\right)^p \tag{2}$$

where u is the wind velocity [m/s] at a height z above the sea level [m], u_0 is the reference wind velocity (set to 7.5 m/s) defined at a height z_0 (set to 10 m), and p was set to 0.13, which is the same value as used for example by Rahimpour and Oshkai [12]. The resulting wind speeds can be seen in Figure 12.

For the wind profile to properly develop, the top of the domain was given a free-slip boundary condition (non-penetrable wall with no friction). The ship is blocking less than 5 % of the cross-section area of the domain, and the sides of the domain were set to a zero-gradient boundary condition. The representative wind and numerical approach were developed for simulations presented in D09.2 “Developed ro-ro spaces fire detection solutions and recommendations“ [13].

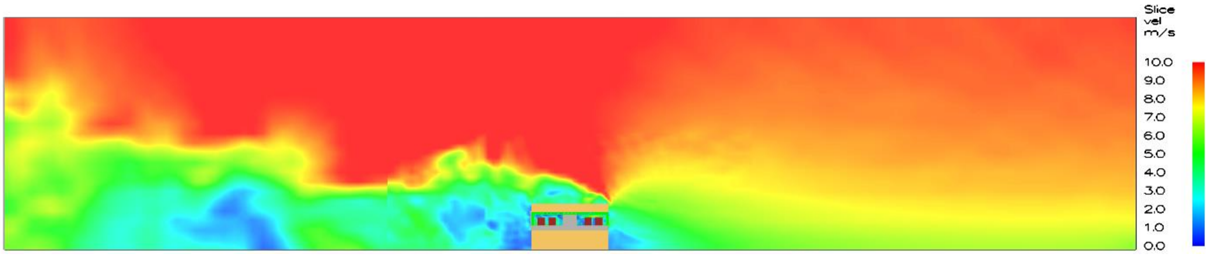

Figure 12: Wind speeds in a view from the rear of the ship. The wind is traveling from the right to the left with a speed of 7.5 m/s at 10 m above sea level. The total hight shown in the figure is 76.8 m.

8.3.6 Modelling of the fire

In the choice of a fire scenario, the fuel and oxygen availability were considered. Before selecting a heat release rate fire curve to be used in the simulations, some hand calculations were made to find out approximately how large fires can be sustained by the access of oxygen.

For the closed ro-ro space, the total volume of the space without cargo was approximately 20 000 m^3. If it is assumed that all oxygen is consumed from the ambient volume fraction of 21 % oxygen in air down to 11 %, and an energy release of 13.1 MJ per consumed kg of air, the total energy released would be 34 GJ. With the fans on and a ventilation of 10 ACPH, the oxygen could sustain a fire with an HRR of approximately 100 MW. The open ro-ro space could get a higher air flow and sustain a much higher HRR than the closed ro-ro space.

A design fire was chosen from tests conducted by Cheong et al. 2012. From that study, test number 7, seen in Figure 4, was chosen, which was a free burning reference case of an HGV in a road tunnel [7]. The fire has a rapid initial growth up to 120 MW. That initial part was used for this study and was then kept at a constant HRR of 120 MW to account for the continued fire spread to adjacent trucks, that will undoubtedly occur at this fire size as long as there is oxygen available, as seen in Figure 13.

The amount of fuel available in a ro-ro space loaded with HGV, assuming that the energy content is similar to the tests in section 7, will be enough for the fire of this size to continue burning under ventilation-controlled conditions for hours.

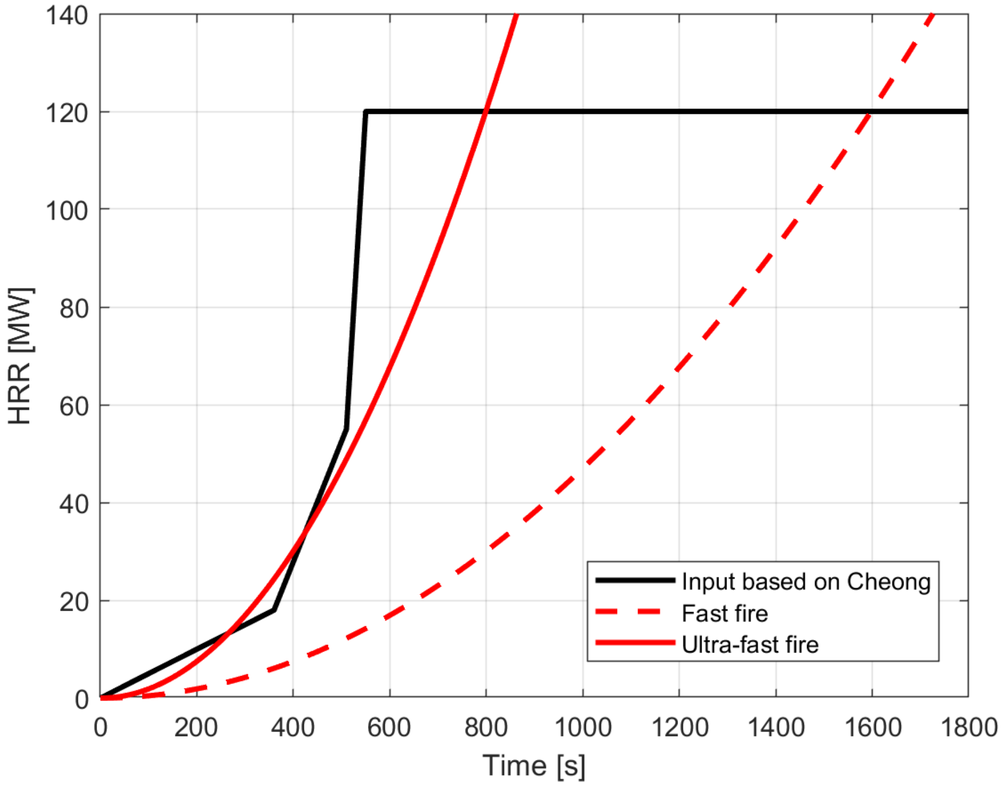

Figure 13: HRR curve used in simulations based on Cheong test 7, compared to the fast and Ultra-fast fire growth rates.

Due to depletion of oxygen, the HRR level will leave fuel unburnt in the simulation model of the closed ro-ro space.

For the open ro-ro space, both fuel (in form of HGVs) and oxygen are enough to sustain a higher HRR than 120 MW. The selected level of 120 MW, representing one truck burning, should therefore be considered as low, keeping in mind that during fire spread from one truck to the other, several trucks would likely be involved at the same time.

8.3.7 Position of the fire origin

The fire source was set to an area elevated 1.2 m above the deck with the dimensions 10 m x 6 m. The reduced height of the burning truck can be considered to represent a late stage of the fire scenario and facilitates the influx of oxygen to the fire. The area is selected to give a realistic maximum heat release rate per unit area (HRRPUA) of 2 MW/m^2.

8.3.8 FDS virtual sensors

The aim of the simulations was to monitor the maximum temperatures reached during a fire in a ro-ro space and the area that exceeds certain limits. The monitoring was done through a grid of FDS virtual sensors registering the temperature in the grid cells closest to the ceiling in the model. The device measures the temperature in a cell ranging from 0 to 20 cm below the ceiling. One device has been placed in the middle of every ceiling compartment/pocket formed by the transversal and longitudinal beams in the ro-ro spaces’ ceilings. The layout can be seen in Figure 14.

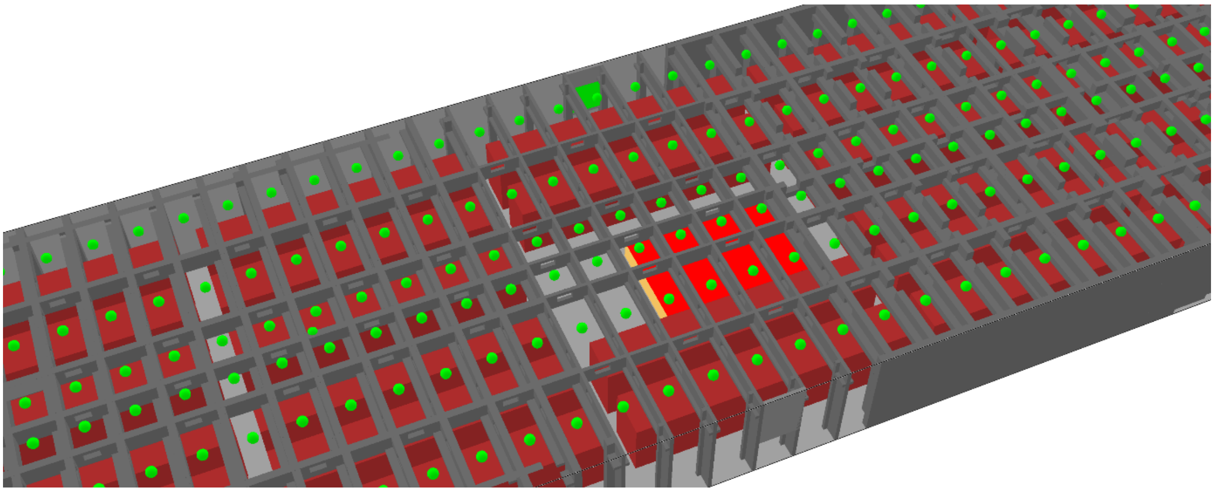

Figure 14: The green dots in the ceiling pockets formed by the transversal and longitudinal ceiling beams are temperature measurement devices.

A horizontal plane spanning the whole deck at 10 cm (0 – 20 cm) below the ceiling have been created for monitoring. For this plane, the total area that exceeds some certain threshold temperatures have been collected and presented in the result section.

8.4 Results of fire simulations

The fire scenarios for the closed ro-ro space, both for the case with no ventilation and with a ventilation of 10 ACPH, became ventilation controlled. For the open ro-ro space, the side and rear openings were enough to supply the 120 MW fire with sufficient oxygen to make it fuel controlled. The actual combusted HRR in the domain during simulations can be seen in Figure 15. For the closed ro-ro space without ventilation, the fire started to deviate from the input curve at around 80 MW and was almost completely extinguished after 700 s. The total energy consumed was 24 GJ. The closed ro-ro space with 10 ACPH reached a stable HRR at approximately 100 MW and during the 30 min of simulation, the total consumed energy was 140 GJ. This value was close to the estimated values from earlier conducted hand calculations in section 8.3.6.

The scenarios for the open ro-ro spaces (wind and no wind) reached their threshold 120 MW and the total energy consumed during 30 min was 180 GJ.

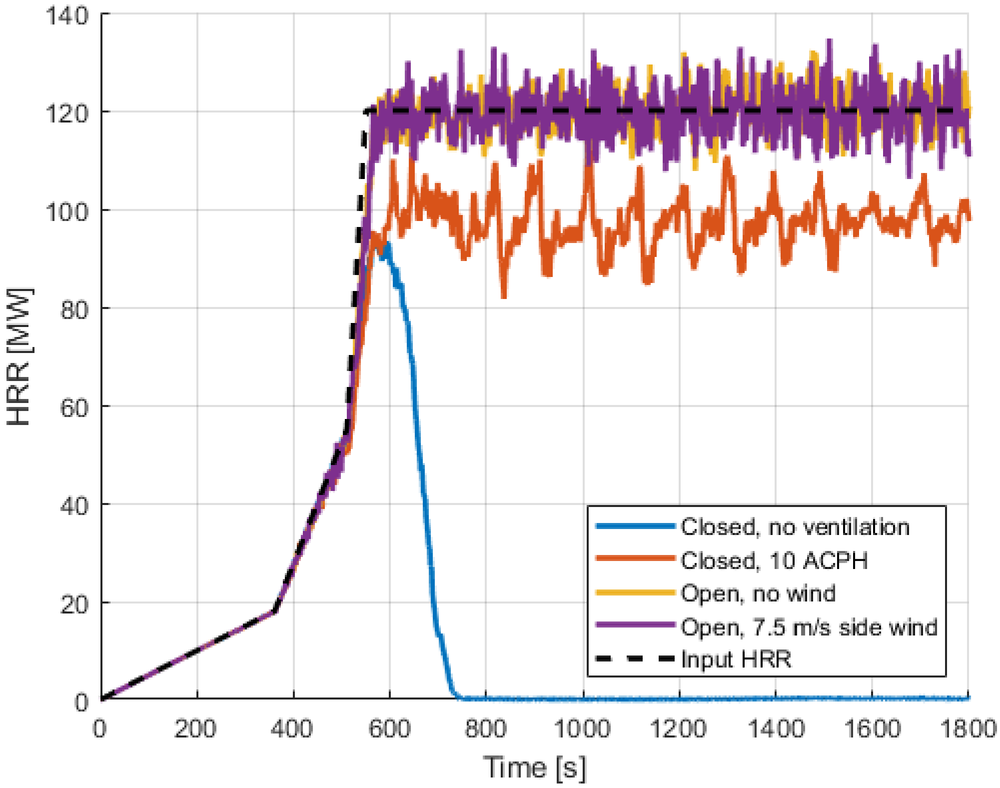

Figure 15: The actual combusted HRR in the simulations in comparison to the input HRR.

Images of air velocities within the ro-ro spaces before ignition are presented below. Figure 16 and Figure 17 show the velocities in the closed ro-ro space with 10 ACPH at two different hights: 2.8 m (between HGVs) and 4.6 m (above HGV). An air velocity of approximately 0.5-1.5 m/s is seen in the majority of the area, and locally, close to the ventilation openings, up to 2 m/s. Figure 18 shows the air velocity for a side wind of 7.5 m/s towards the side of the open ro-ro space. An air velocity between 1.0 - 3.5 m/s can be seen in most of the area, with velocities up to 4.5-5.0 m/s close to the openings at the side facing the wind.

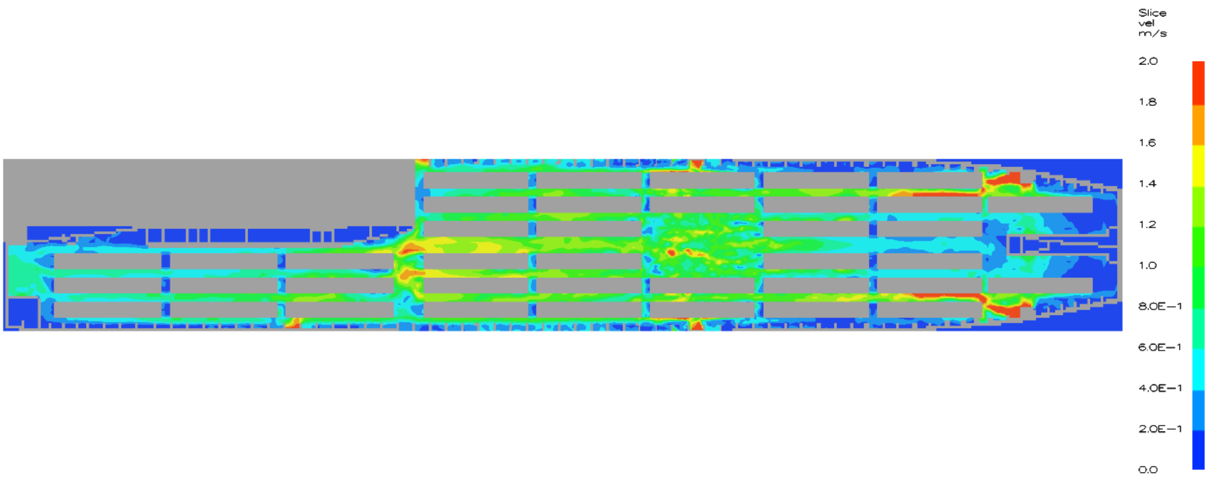

Figure 16: Closed ro-ro space with mechanical ventilation turned on (10 ACPH). Visualization of the air speed at a height of 2.8 m above deck, which is half the ceiling height. The figure is taken right before ignition. Dark red means a wind speed over 1.8 m/s.

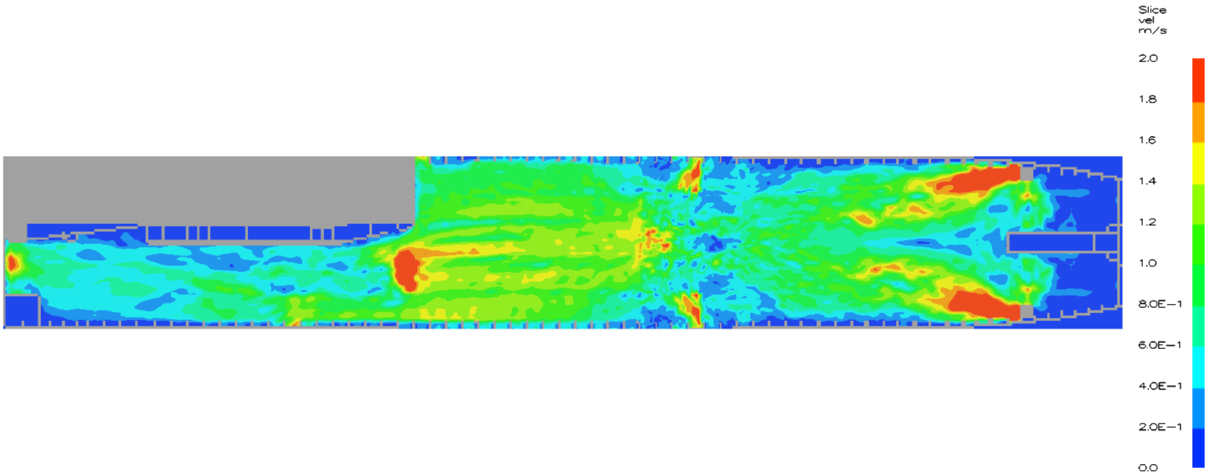

Figure 17: Closed ro-ro space with mechanical ventilation turned on (10 ACPH). Visualization of the air speed at a height of 4.6 m above deck, which is right below the framework. The figure is taken right before ignition. Dark red means a wind speed over 1.8 m/s.

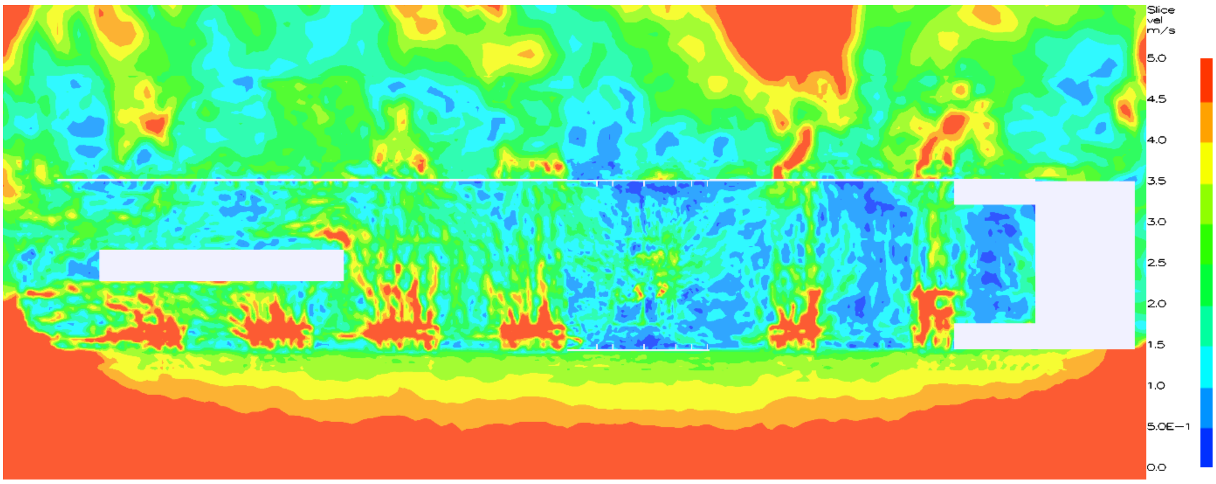

Figure 18: Open ro-ro space with wind. Visualization of the air speed at a height of 4.8 m above deck, which is right below the beam framework. The figure is taken 2 min after ignition, when the fire has developed to 5 MW. Dark red means a wind speed over 4.5 m/s. Note, upper and lower third of the figure shows the wind condition outside the ship.

In the following section, when analysing the results, two aspects are important to keep in mind:

1. To model the fluid dynamics and chemical combustion in a flame accurately would require a fine grid in the scale of centimetres or even millimetres. For a scenario of the size of a room, or these ro-ro spaces, FDS provides a simplified combustion model, and it is a well-known fact that temperatures calculated in a flame may deviate from the reality. The temperatures presented in volumes of a flame should be considered as relative values. Temperatures in the smoke gases are more accurate [14].
2. When presenting the areas exposed to different temperatures, it should be remembered that for open ro-ro spaces and for closed ro-ro spaces with 10 ACPH, the continuing high HRR level (Figure 13) necessitates a continuing fire spread involving several trucks. For this high HRR level, this is a realistic assumption, but in a real scenario it would result in the fire source

moving and widening and not staying in one location as is the case in the simulation models. Nevertheless, the presentations of areas being affected are still interesting information and should be analysed keeping this in mind.

8.4.1 Smoke gas temperature in closed ro-ro space

For the closed ro-ro space without ventilation, the maximum temperatures were reached 10 min after ignition, see Figure 19, which is the same time as the maximum HRR was reached. After that, the temperatures dropped due to lack of oxygen supply. Right above the fire source, some computational cells reached temperatures close to 1 000°C for a short moment. Some detectors noticed a higher temperature than the ISO 834 curve for approximately 4 min, see Figure 20. The temperature, however, never reached the Hydrocarbon curve for a single position over the simulation’s duration. The area which reached high temperatures for this scenario was quite small. The maximum area that reached a temperature over 600°C was 160 m^2 and only 40 m^2 ever reached more than 800°C, as shown in Figure 21.

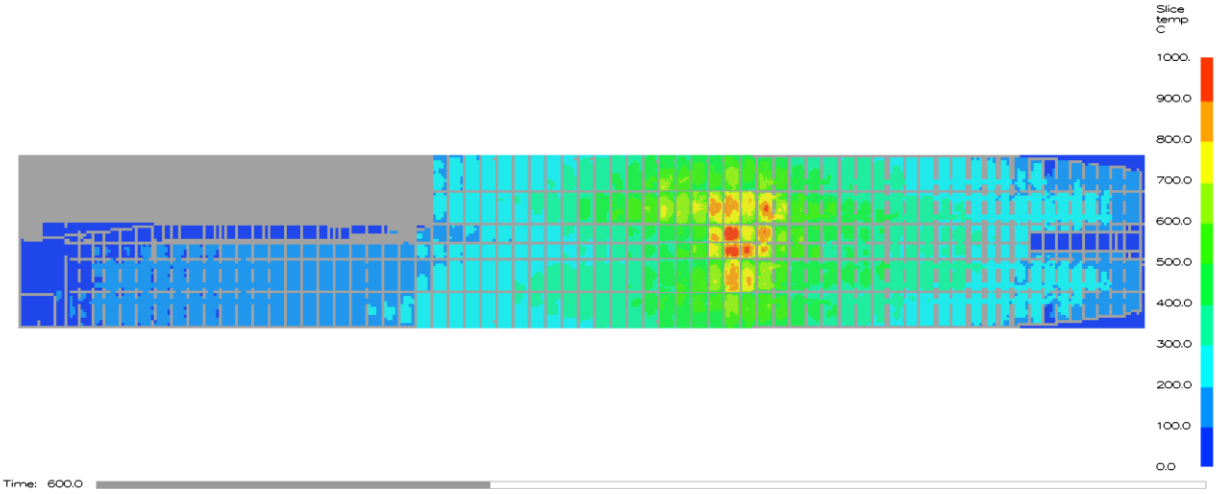

Figure 19: The temperatures in the grid cell 0 – 20 cm below the ceiling for the closed ro-ro space and without any ventilation at 10 min after the simulation started.

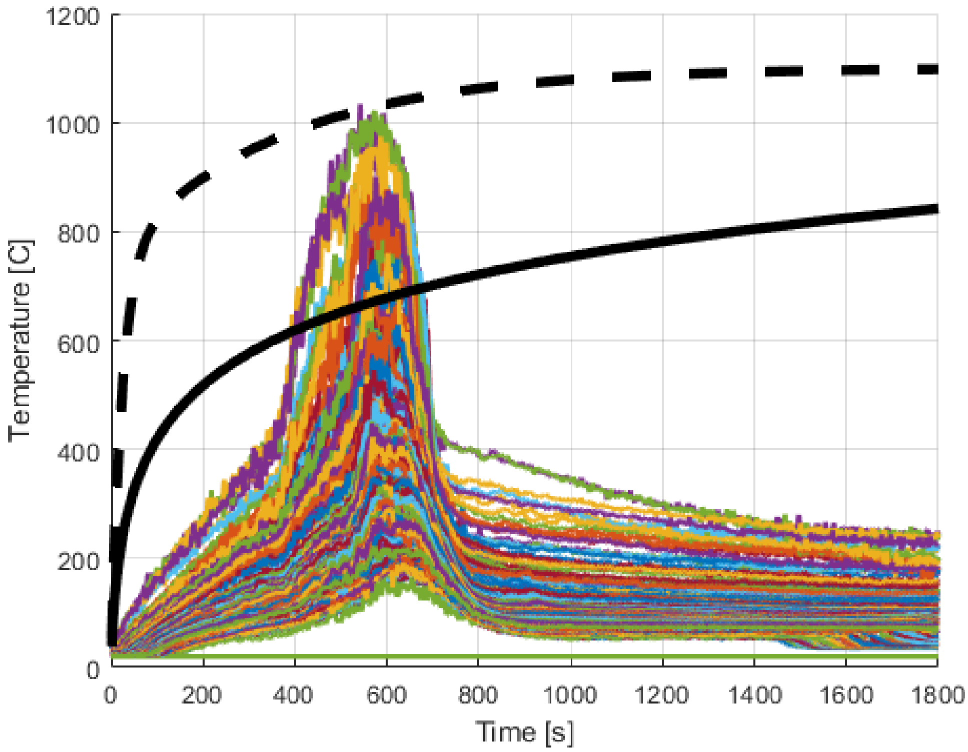

Figure 20: Closed ro-ro space without ventilation. Gas temperatures at each device located just below the ceiling. The black dashed line is the Hydrocarbon curve, and the black solid line is the ISO 834 fire curve.

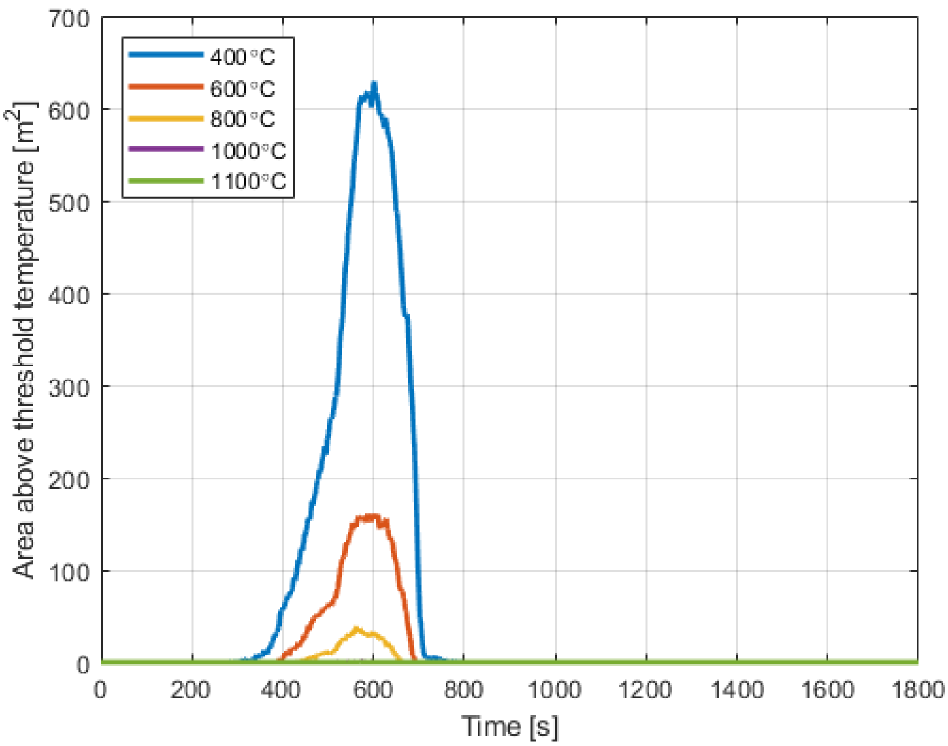

Figure 21: Closed ro-ro space without ventilation. The total area of the air 0 – 20 cm below the ceiling that exceeds a threshold temperature.

For the closed ro-ro space with a ventilation of 10 ACPH, the temperatures increase over time. Even if the detected maximum temperature of 1 000°C was approximately the same as in the scenario without ventilation, it was here reached at the end of the simulation. The temperatures after 30 min can be seen in Figure 22. The temperature for the warmest devices right above the fire source will show temperatures between the ISO 834 curve and the hydrocarbon curve, as seen in Figure 23. After 30 min had elapsed, a ceiling area of 340 m^2 and 70 m^2 had a temperature above 600°C and 800°C, respectively, as seen in Figure 24.

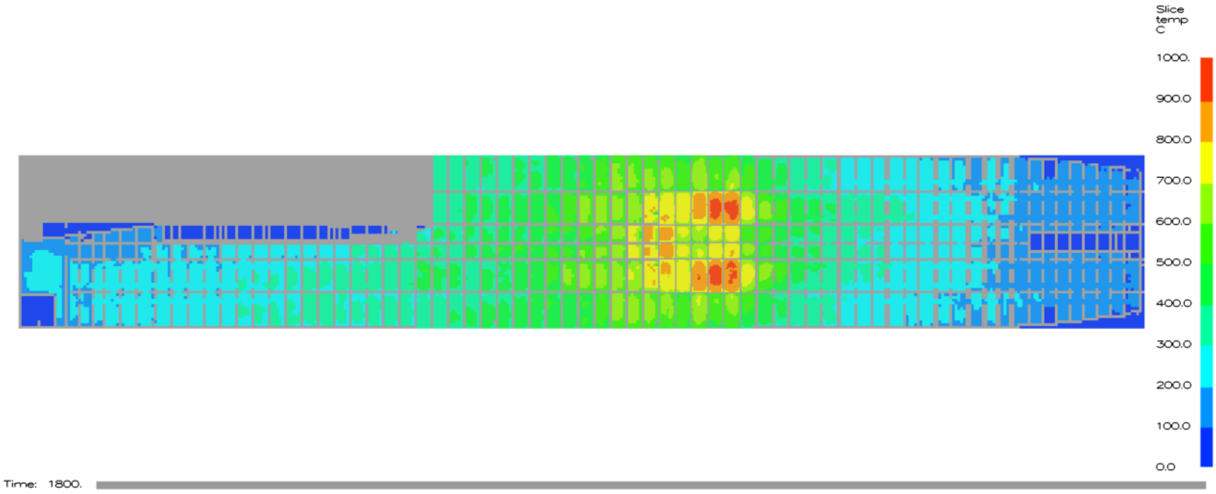

Figure 22: The temperatures in the grid cell 0 – 20 cm below the ceiling for the closed ro-ro space with a ventilation of 10 ACPH at 30 min after the simulation started.

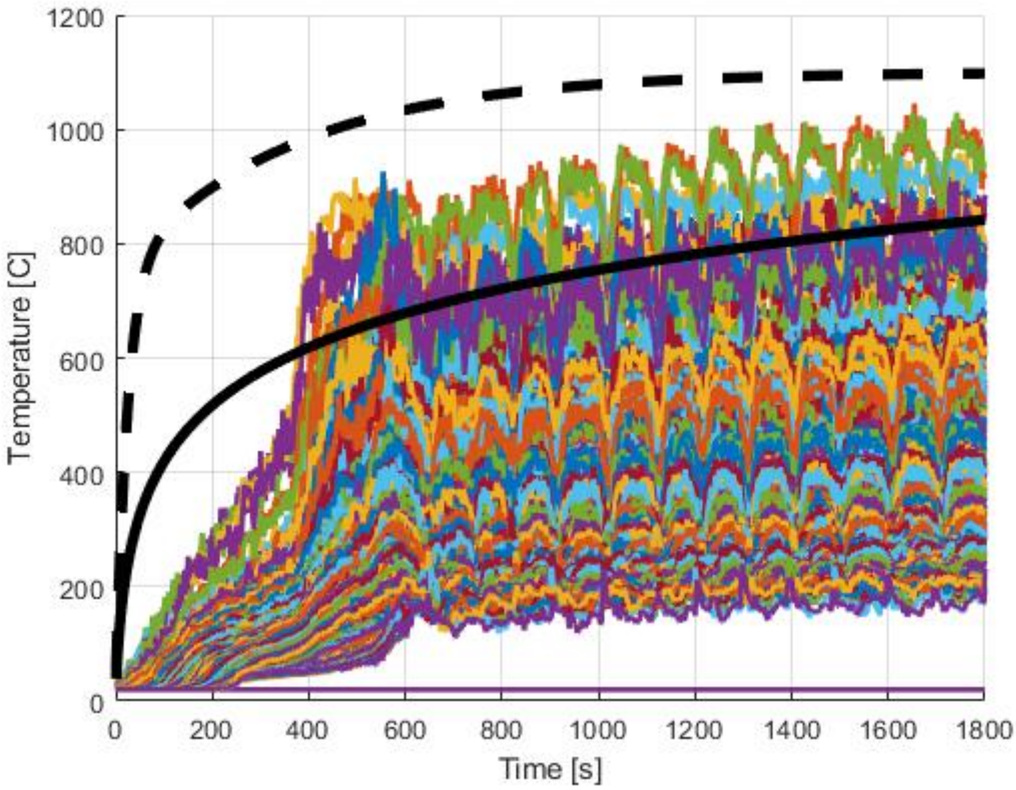

Figure 23: Closed ro-ro space with a ventilation of 10 ACPH. Gas temperatures at each device located just below the ceiling. The black dashed line is the Hydrocarbon curve, and the black solid line is the ISO 834 fire curve.

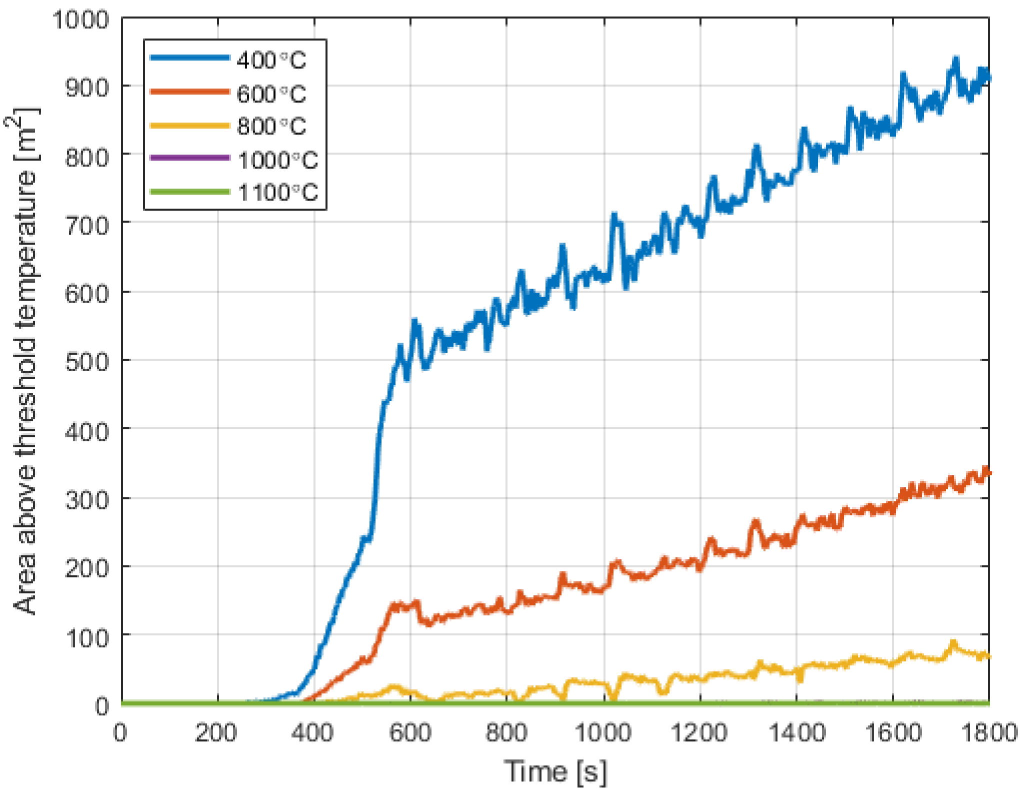

Figure 24: Closed ro-ro space with a ventilation of 10 ACPH. The total area of the air 0 – 20 cm below the ceiling that exceeds a threshold temperature.

8.4.2 Smoke gas temperatures in open ro-ro space

The gas temperatures reached in the open ro-ro space without wind were considerably higher than for the closed ro-ro space, see Figure 25. The maximum temperatures detected were above 1 300°C. The absolute temperatures in the flames should however be read with caution, but it was noted that the temperatures were in the region of what was measured in real tunnel fire tests. The simulated temperatures exceeded the temperatures of the Hydrocarbon curve at some of the devices, see Figure 26. At 10 min, the temperatures started to reach 1 100°C closest to the fire source. This develops to an area of 30, 75, 130, and 200 m^2 after 15, 20, 25, and 30 min from ignition, respectively.

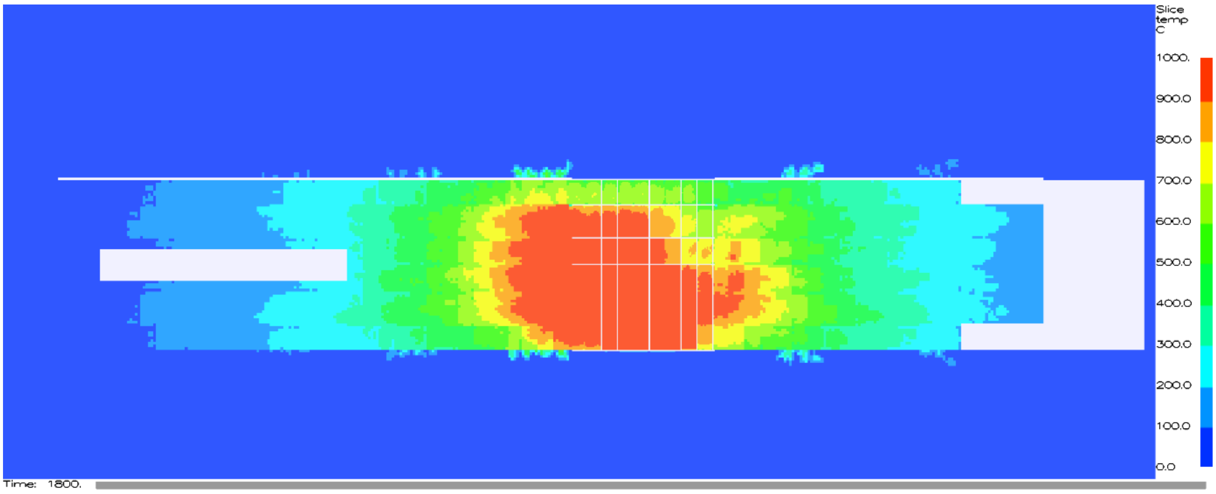

Figure 25: The temperatures in the grid cell 0 – 20 cm below the ceiling for the open ro-ro space without any wind at 30 min after the simulation started.

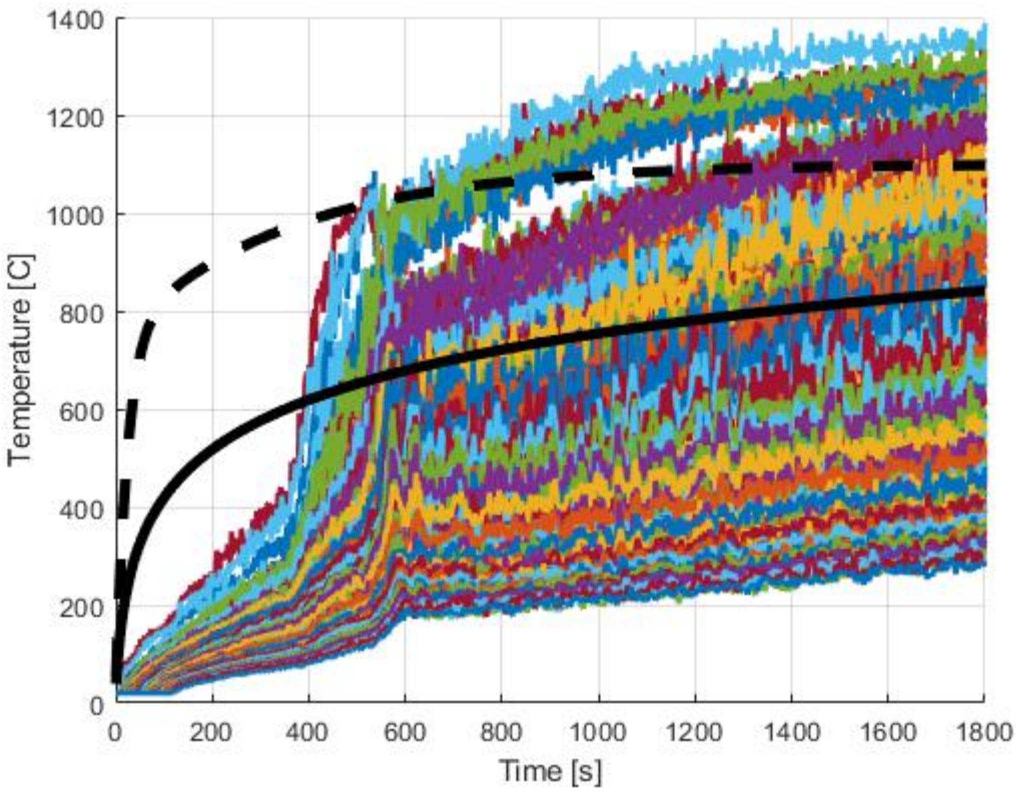

Figure 26: Open ro-ro space without wind. Gas temperatures at each device located just below the ceiling. The black dashed line is the Hydrocarbon curve and the black solid line is the ISO 834 fire curve.

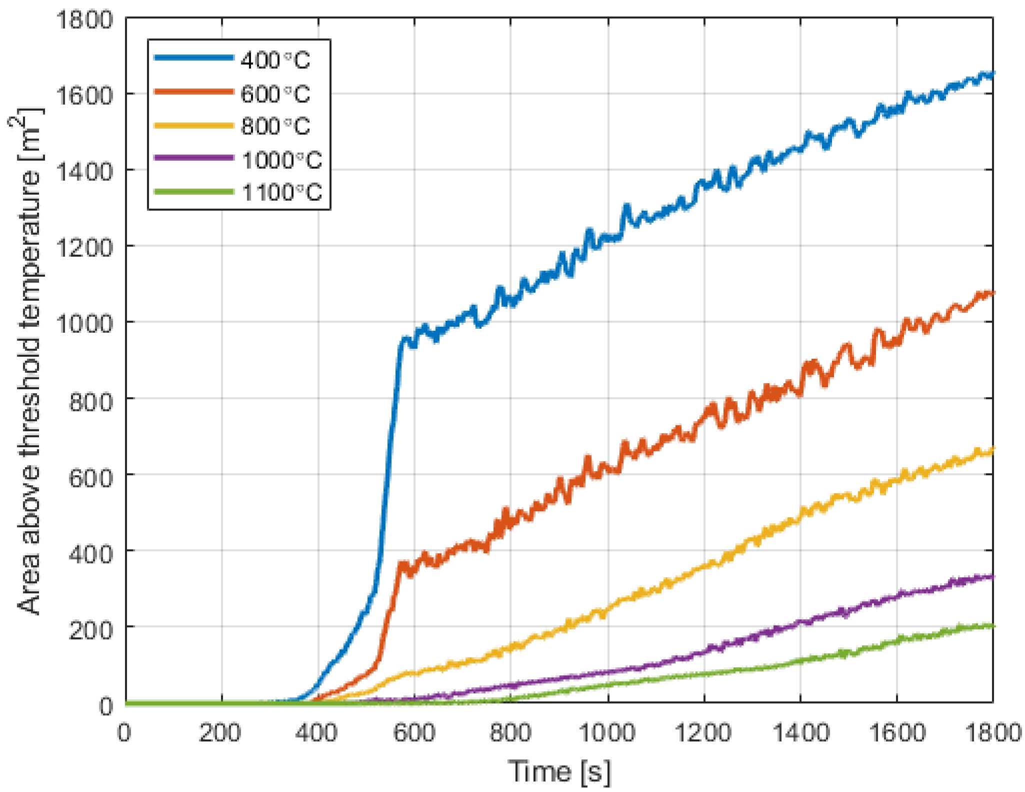

Figure 27: Open ro-ro space without wind. The total area of the air 0 – 20 cm below the ceiling that exceeds a threshold temperature.

The temperatures for the open ro-ro space with a 7.5 m/s side wind were similar to the ones for the open ro-ro space without wind, see Figure 28. The maximum temperatures detected were above 1 300°C. Once again, the absolute temperatures in the flames should be read with caution but also for this scenario the temperatures reached the region observed in the real fire tests. As seen in Figure 29, some of the detectors measure temperatures that exceed the hydrocarbon curve after 12 min after ignition. At 10 min, the temperatures started to reach 1 100°C closest to the fire source. This developed to an area of 12, 60, 160, and 250 m^2 after 15, 20, 25, and 30 min from ignition, respectively.

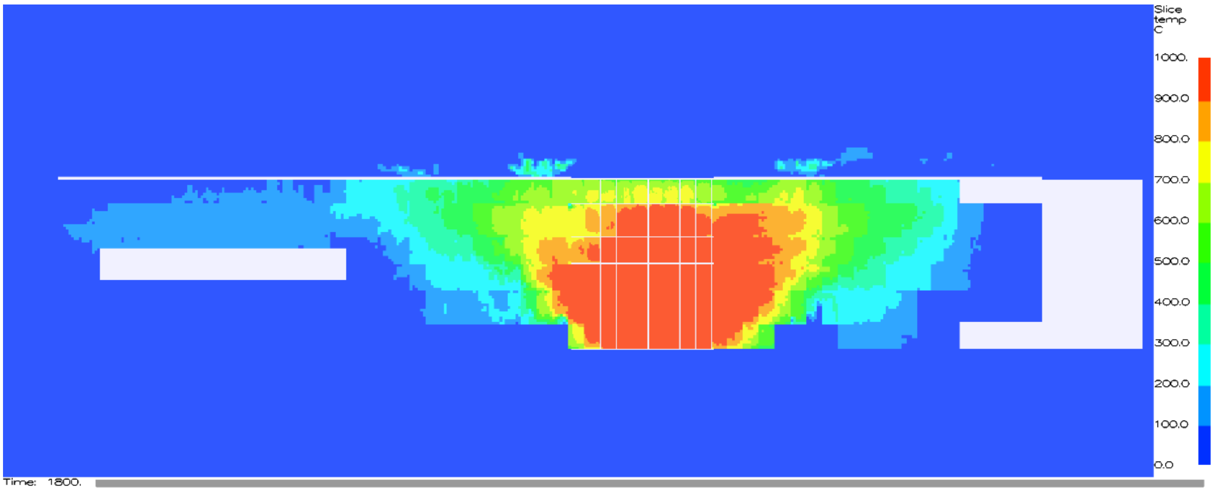

Figure 28: The temperatures in the grid cell 0 – 20 cm below the ceiling for the open ro-ro space with a side wind of 7.5 m/s at 30 min after the simulation started.

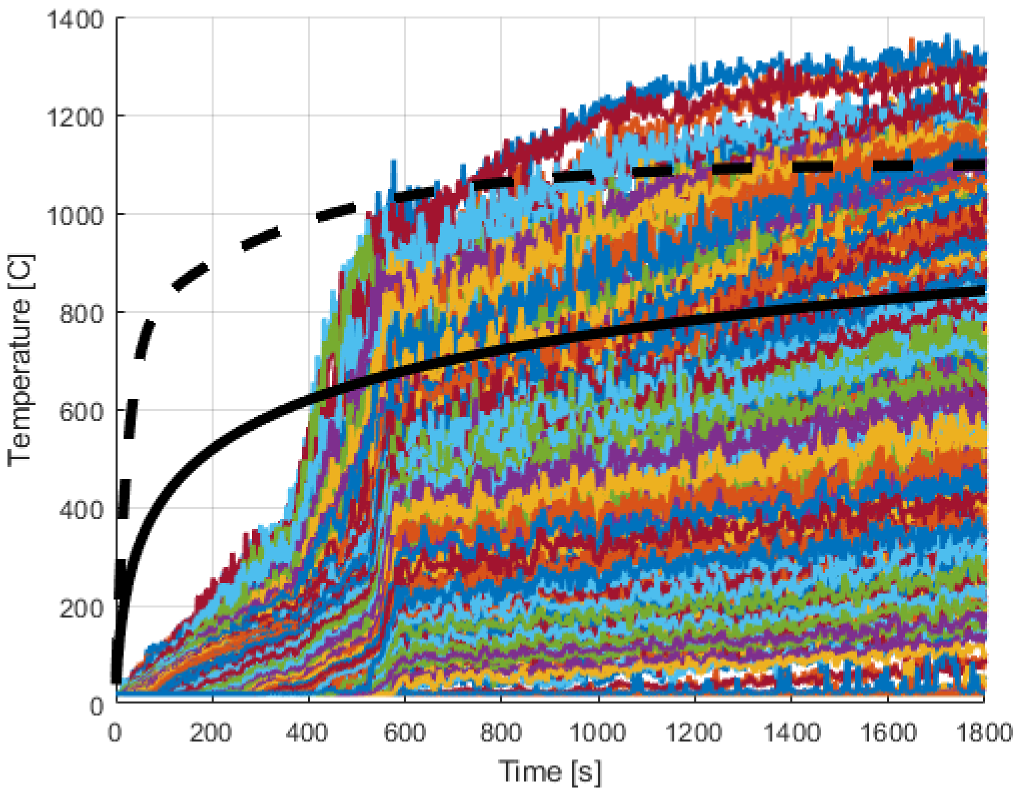

Figure 29: Open ro-ro space with 7.5 m/s side wind. Gas temperatures at each device located just below the ceiling. The black dashed line is the Hydrocarbon curve and the black solid line is the ISO 834 fire curve.

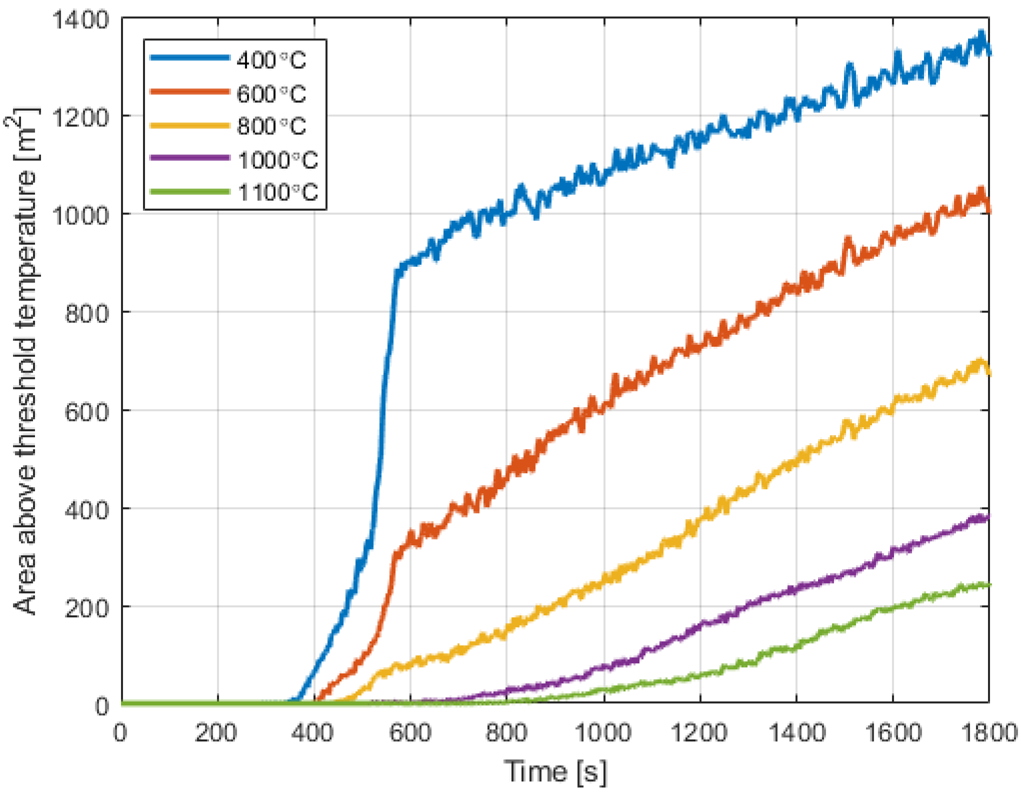

Figure 30: Open ro-ro space with 7.5 m/s side wind. The total area of the air 0 – 20 cm below the ceiling that exceeds a threshold temperature.

9 Determination of relevant heat exposure to use during fire resistance testing

Main authors of the chapter: Maria Hjohlman

The determination of a realistic heat exposure was based on comparisons of the measured temperature (from fire tests) and the calculated temperatures (from numerical simulations) with time-temperature curves usually used in fire resistance testing, presented in Figure 1. The results presented in previous sections show that the exposure level is dependent on the openness of deck space and ventilation conditions.

9.1 Open ro-ro space

For fires in open ro-ro spaces, the following scenarios and figures are of relevance:

- Tunnel fire tests of (a single) HGV, Figure 5.
- Simulations of HGV fire in open ro-ro space with a sidewind of 7.5 m/s, Figure 29.
- Simulations of HGV fire in open ro-ro space without sidewind, Figure 26.

A temperature comparison of all three cases shows that the HC curve gives a better representation of the realistic heat exposure than the ISO 834 curve.

From the graphs comparing measured and simulated temperatures for ro-ro spaces fully loaded with trucks and time-temperature curves, it is apparent that the HC curve gives a better representation than the ISO 834 curve. Indeed, within 7 minutes of the simulated fire, the temperatures encountered were higher than the ISO 834 time-temperature curve temperature. It is also shown that the heat exposure is not only local; on the contrary, the high heat will affect a large area involving several ceiling pockets formed by the transversal and longitudinal bulkhead beams.

The heat exposure in case of a fire in an open ro-ro space loaded with trucks would therefore be better represented by the HC curve.

9.2 Closed ro-ro space

For fires in closed ro-ro spaces, the following scenarios and figures are of relevance:

- Simulations of HGV fire in closed ro-ro space with a ventilation of 10 ACPH, Figure 23.
- Simulations of HGV fire in closed ro-ro space with ventilation turned off, Figure 20.

For the case with a ventilation of 10 ACPH in the closed ro-ro space, the heat exposure during the fire involving HGVs reached above the ISO 834 curve. The temperatures reached a level between the ISO 834 curve and the HC curve in a considerably large area (approximately estimated to 70 m^2 from Figure 22 to Figure 24). After approximately 7 minutes, the temperature in the ceiling area closest to the fire had reached 100-200 degrees above the ISO 834 curve and continued to rise, following the same growth rate as the ISO 834 curve, steadily approaching the HC curve.

Due to the temperatures being considerably above the ISO 834 curve in a relatively large area, the heat exposure in case of a fire in a closed ro-ro space loaded with trucks would be better represented by the HC curve.

For a closed ro-ro space with no presence of openings and with the ventilation turned off, the depletion of oxygen causes the HRR and temperature curves to drop after approximately 7 minutes. In some areas right above the fire source, a higher temperature than the ISO 834 curve was reached for approximately 4 min, see Figure 20.

Since the limited access of oxygen quickly reduced the size of the fire, the ISO 834 curve is judged to be a reasonable representation of the heat exposure. In a real scenario, some leakage can be expected, but they were assumed to be low enough to keep the temperatures well below the ISO 834 curve.

The simulated closed ro-ro space in this study had no openings and with ventilation turned off it was regarded as being completely sealed. The good effect of the depletion of oxygen seen in the case of no ventilation would not occur at the same early stage if openings were present. As is described in section 4.1.2.2, the definition of a closed ro-ro space covers all cases where a ro-ro space is not open enough to be considered as an open ro-ro space or a weather deck, which implies required mechanical ventilation. Openings may be present; the space can for example be open in one end. The conclusion that the HC curve is representative for the heat exposure in the event of a fire in a closed ro-ro space with ventilation on is valid also in the presence of openings, for obvious reasons.

The scenario with a closed ro-ro space with openings, such as with one end open, was not investigated in this study. The outcome would depend on the size and location of the openings in relation to the fire source and other conditions such as the presence and direction of wind. This conclusion is also supported by the RISE project RO5 [8] where the influence of openings and ventilation on a fire in a closed ro-ro space were studied using model scale fire tests and numerical simulations. The amount of fresh air that reaches to the fuel source determines the intensity of the fire. For 4% side openings, and no mechanical ventilation, the tests showed a distinct limitation of the fire, but it was further concluded that the way fresh air is transported and mixes on the way from the supply (opening or duct) towards the fire is crucial for the survival of the fire.

9.3 Summary of relevant heat exposure

For the present study, the definition of a realistic heat exposure resulting from a cargo fire in a ro-ro space consists of selecting the time-temperature curve which best represents the temperatures found from fire tests and simulated by FDS. Based on the previous paragraph, the heat exposure recommended to be used for fire engineering and testing purposes is presented in Table 8.

Table 8. Time-temperature curves best representing realistic heat exposure resulting of cargo fire in ro-ro space

Type of ro-ro space	Ventilation condition	Representative standard fire curve
Open space	Natural	Hydrocarbon curve
Closed space with no openings (almost sealed)	Mechanical ventilation is guaranteed to be turned off	ISO 834 curve
Closed space with no openings (almost sealed)	Mechanical ventilation can not be guaranteed to be turned off	Hydrocarbon curve
Closed space with openings	Mechanical ventilation can not be guaranteed to be turned off	Hydrocarbon curve
Closed space with openings	Natural (Mechanical ventilation is guaranteed to be turned off)	Not determined

10 A-class fire protection in regards of a realistic fire

Main authors of the chapter: Pierrick Mindykowski (RISE)

It is demonstrated in previous sections that the heat exposure from a realistic fire within an open ro-ro space and a closed ro-ro space with ventilation kept on is better represented by the HC time-temperature curve than the ISO 834 time-temperature curve, which is currently used to approve thermal insulation on ships, according to the FTP Code.

10.1 Experimental tests

Using the same criteria for the approval of A class thermal insulation defined by SOLAS, a set of experiments were performed to judge the likely fire integrity of an A class thermal insulation when exposed to the hydrocarbon time-temperature curve in a small cubic furnace.

10.1.1 Presentation and procedure of the experimental tests

The experimental tests conducted for this part of the study were based on standard tests according to the FTP Code. An already approved thermal insulation was mounted on a steel plate and placed horizontally on a cubic furnace with the dimensions: 1.2m x 1.2m x 1.2m. It should be noted here that this cubic furnace is smaller than a standard furnace used for type approving material. The furnace is shown in Figure 31 and Figure 32.

Figure 31. Picture of the furnace used for the testing (top view).

Figure 32. Picture of the furnace used for the testing (front view).

The thermal insulation was mounted on steel plate as described in Figure 33.

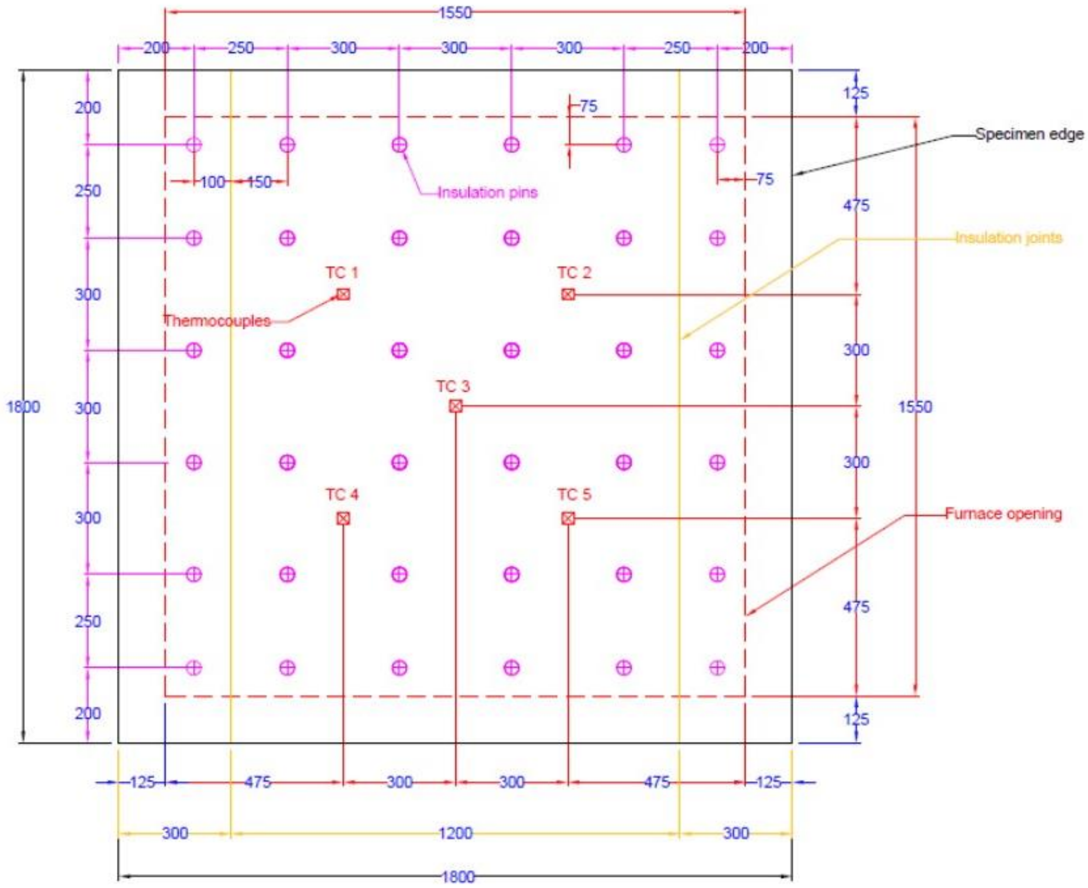

Figure 33. Presentation of the mounting of the thermal insulation on the steel plate.

The position of the thermal insulation with regards to the furnace is shown in Figure 34.

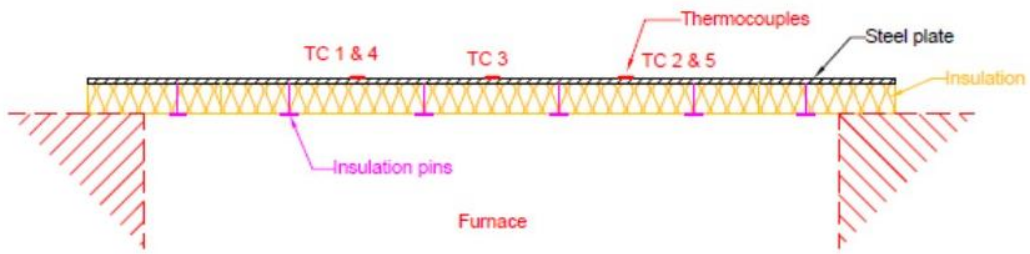

Figure 34. Position of the thermal insulation on the furnace.

The testing procedure consisted of the following:

- Mounting the thermal insulation on steel plate
- Positioning the thermal insulation and steel plate on the top of the furnace
- Exposing the thermal insulation to the HC time-temperature curve for 30 minutes or 60 minutes
- Monitoring the increase in temperature at the non-exposed side of the thermal insulation by thermocouple measurements (shown in Figure 33)

10.1.2 Matrix of experimental tests

Concerning thermal insulation, several types are commonly used for protection onboard. For the current study, two types of materials were tested:

- Glass wool
- Stone wool.

Regarding the steel plate, three thicknesses were used:

- 5 mm (as required by the FTP Code)
- 6 mm (used when the ro-ro space is designed for cars)
- 12 mm (used when the ro-ro space is designed for trucks).

The matrix of tests is represented in Table 9.

Table 9. Matrix of the tests

Class of thermal insulation	Type of thermal insulation material	Thickness of the steel plate (mm)	Duration of test (minutes)
A-30	Glass Wool	6	30
A-60	Stone wool	6	60
A-30	Stone wool	6	30
A-30	Stone wool	5	30
A-30	Stone wool	12	30
A-60	Stone wool	12	60

10.2 Results of the experiments

The outcomes of the experiments consisted of the recorded temperatures at the non-exposed side of the thermal insulation in order to compare them to the criteria used in the FTP Code.

10.2.1 A-30 glass wool on 6 mm steel plate

This test was carried out with A-30 thermal insulation made of glass wool mounted on a steel plate of 6 mm. The temperature results are presented in Figure 35.

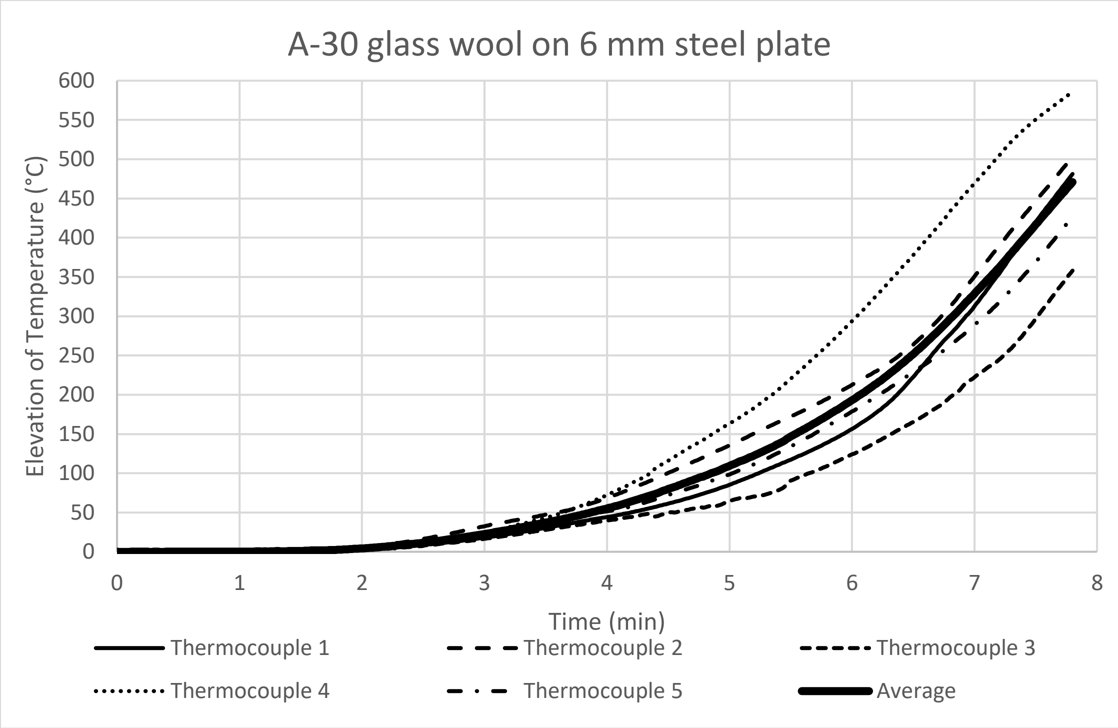

Figure 35. Elevation of temperature for A-30 glass wool on 6 mm steel plate.

This test had to be stopped before the planned end time. At 8 minutes, the elevation of temperatures had already reached around 500 °C. This unexpected high temperature can be explained by the fact that the insulation (glass wool) melted during the test. The final state of the insulation is shown in Figure 36.

Figure 36. Picture of the glass wool insulation after 8 minutes of heat exposure according to the Hydrocarbon time-temperature curve.

Surprised by the results, an additional test was performed with the A-30 glass wool thermal insulation but with heat exposure according to the cellulosic time-temperature curve (ISO 834 according to the FTP Code). Figure 37 shows this thermal insulation after 30 minutes.

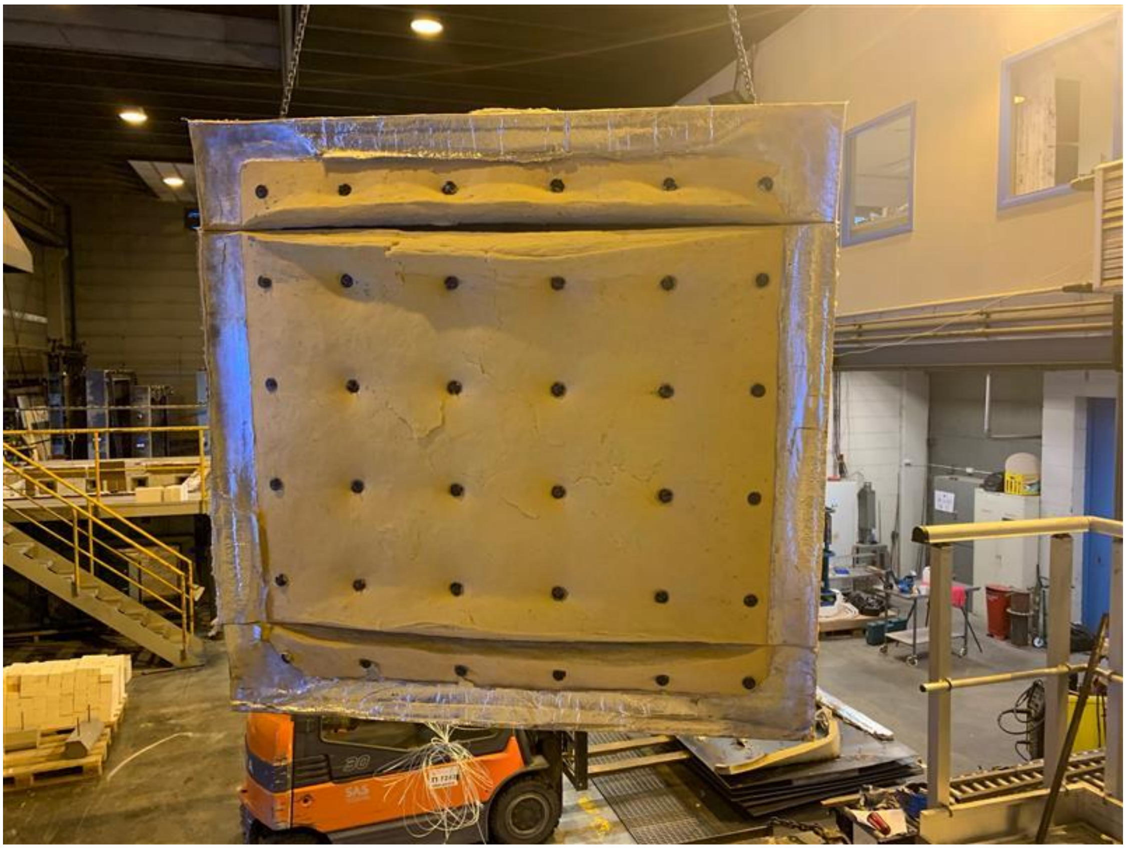

Figure 37. Picture of the glass wool insulation after 30 minutes of heat exposure according to the cellulosic (ISO 834) standard time-temperature curve.

Figure 37 demonstrates that the glass wool thermal insulation can sustain the cellulosic standard time-temperature curve, while it deteriorated when exposed to the more severe Hydrocarbon time-temperature curve.

10.2.2 A-60 stone wool on 6 mm steel plate

This test consisted of A-60 thermal insulation made of rock wool mounted on a steel plate of 6 mm. The temperature results are presented in the Figure 38.

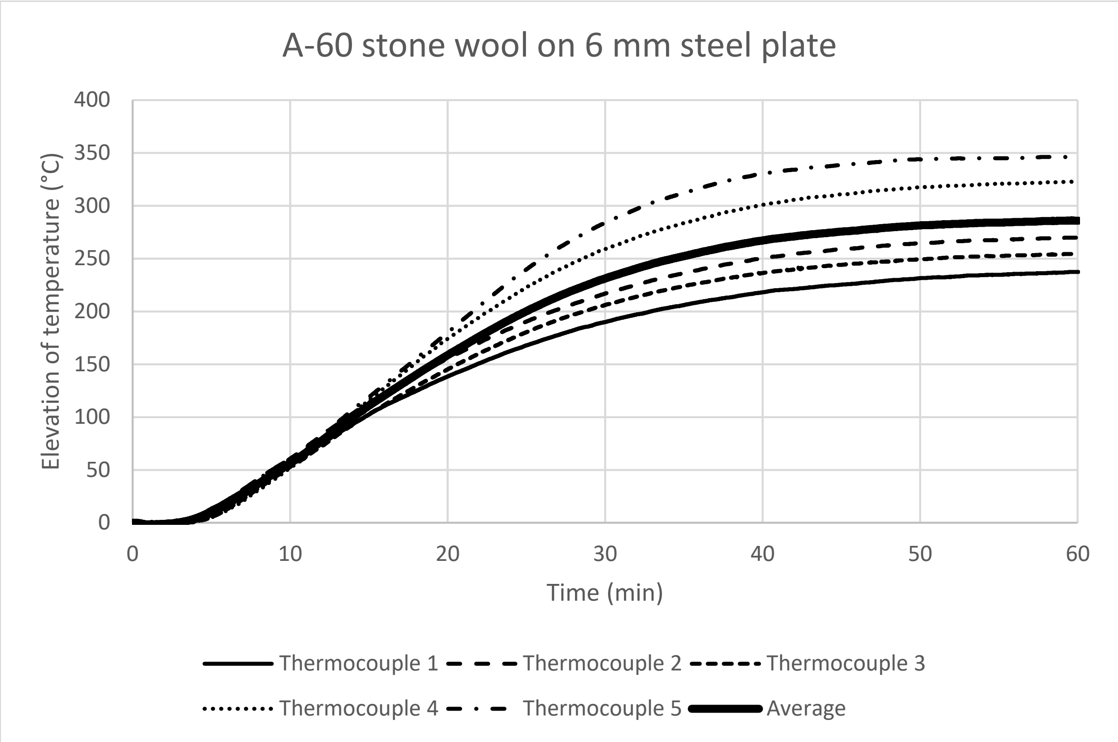

Figure 38. Elevation of temperature for A-60 stone wool on 6 mm steel plate.

A quite homogenous range of temperatures was measured in test consisting of A-60 stone wool mounted on a 6 mm steel plate.

10.2.3 A-30 stone wool on 6 mm steel plate

The third test consisted of A-30 thermal insulation made of stone wool mounted on a steel plate of 6 mm. The temperature results are presented in the Figure 39.

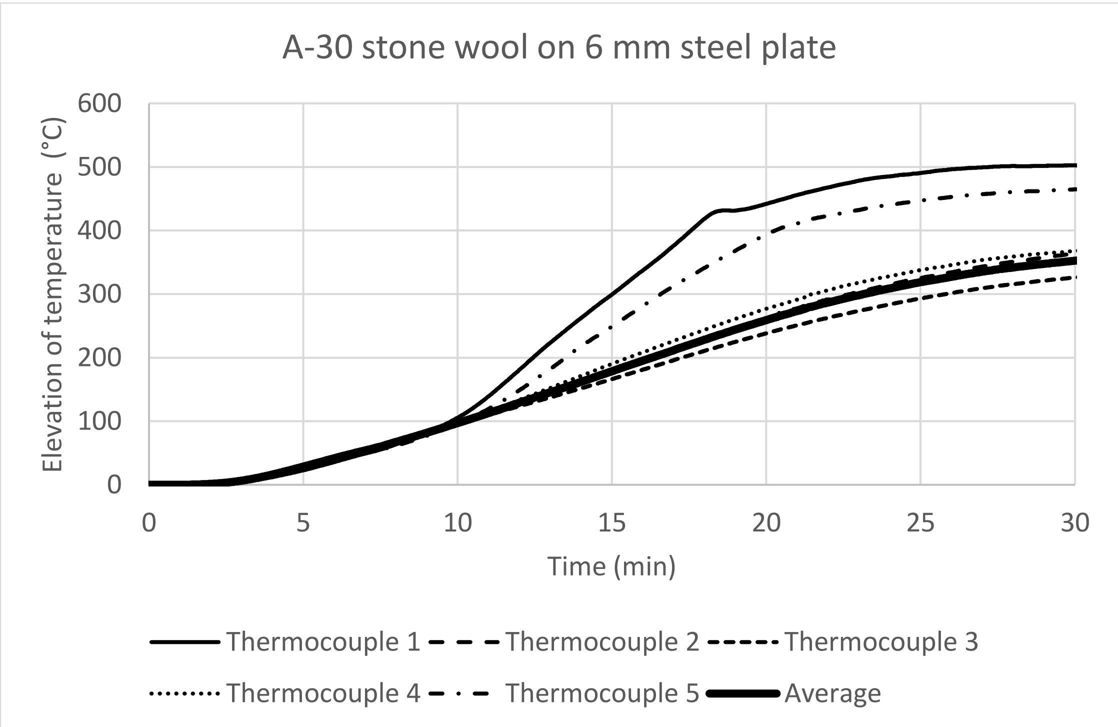

Figure 39. Elevation of temperature for A-30 stone wool on 6 mm steel plate.

For this test, two thermocouples (1 and 5, see Figure 33) seemed to show erroneous behaviour compared to the other three thermocouples. This difference may be explained by the fact that the insulation might have lost its contact with the steel plate, or that the insulation joints (as shown in Figure 33) might have opened up during the test. As no visual observation was made done after this test, the previous explanations are only hypothetical.

10.2.4 A-30 stone wool on 5 mm steel plate

The fourth test consisted of A-30 thermal insulation made of stone wool mounted on a steel plate of 5 mm. The temperature results are presented in the Figure 40.

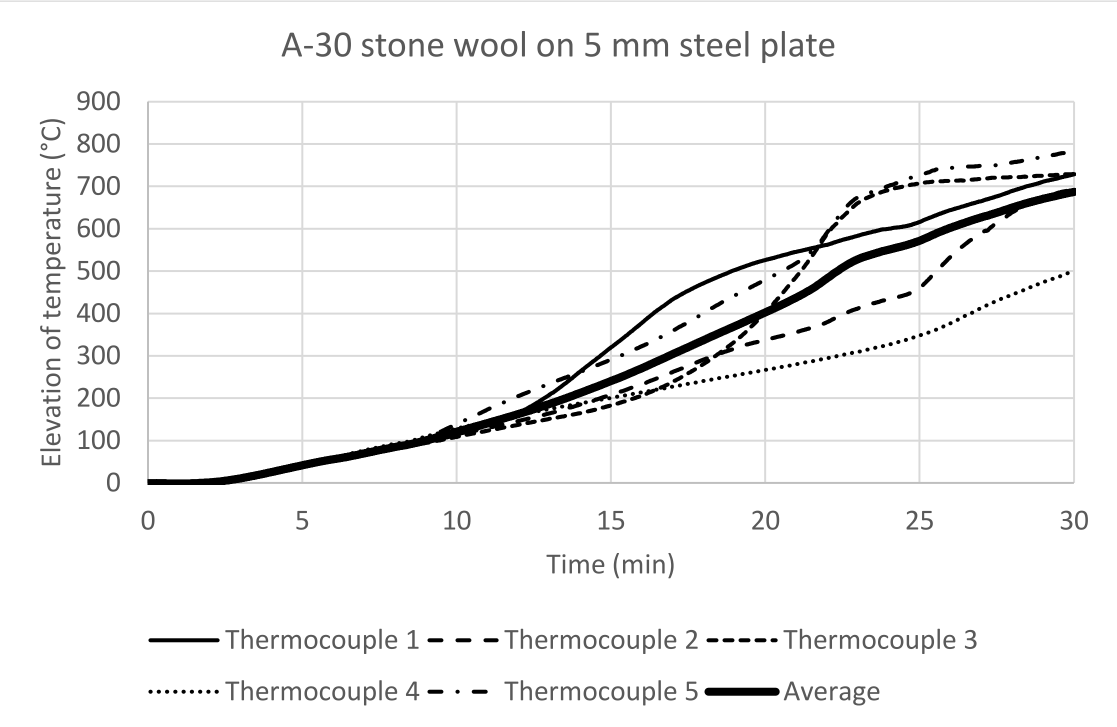

Figure 40. Elevation of temperature for A-30 stone wool on 5 mm steel plate.

In this test, thermocouples 3 and 5 showed a steep increase in temperature around 20 minutes. This behaviour did not influence the final result (as shown in Figure 40) and can be explained by that the insulation did not fully resist the intensity of the heat exposure and started to deteriorate, as shown in Figure 41. It should be noted here that the mounting of the thermal insulation did not follow the installation requirement shown in Figure 33 due to a shortage of insulation.

Figure 41. Picture of the stone wool thermal insulation after a test with A-30 stone wool on a 5 mm steel plate.

10.2.5 A-30 stone wool on 12 mm steel plate

This test consisted of A-30 thermal insulation made of rock wool mounted on a steel plate of 12 mm. The temperature results are presented in the Figure 42.

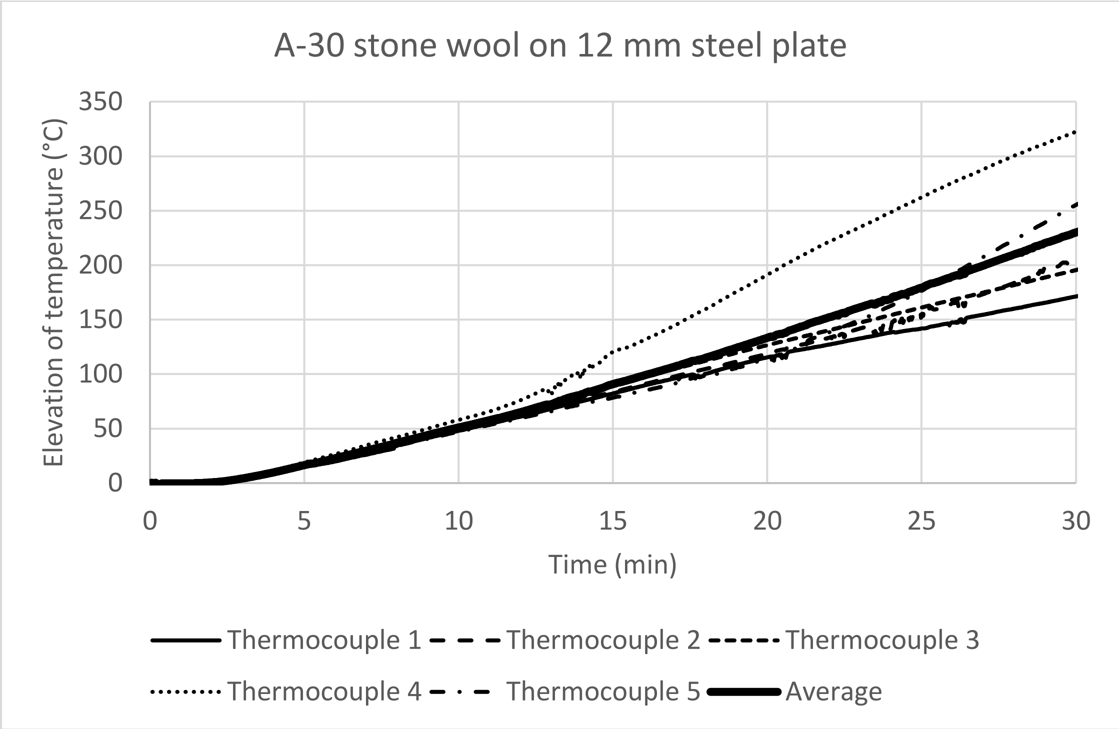

Figure 42. Elevation of temperature in test for A-30 stone wool on 12 mm steel plate.

In this test, thermocouple number 4 showed a different behaviour than the others. It resulted in a relatively high average temperature compared with thermocouples 1, 2, 3 and 5.

10.2.6 A-60 stone wool on 12 mm steel plate

This test consisted of A-60 thermal insulation made of stone wool mounted on a steel plate of 12 mm. The temperature results are presented in the Figure 43.

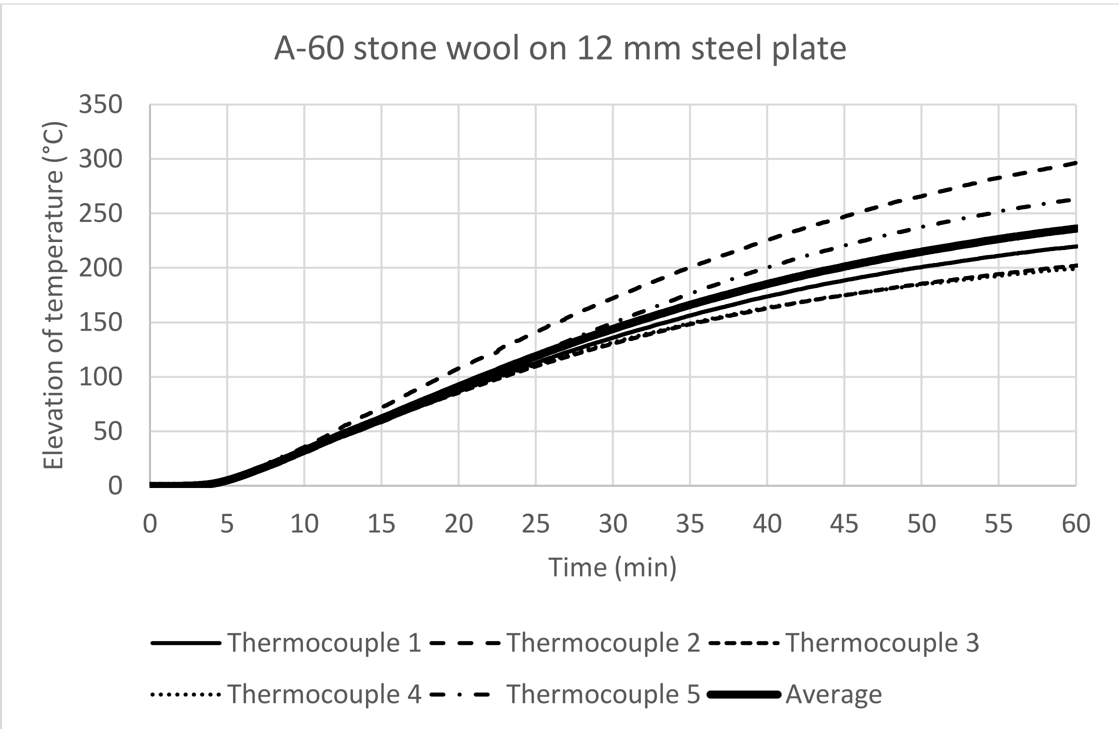

Figure 43. Elevation of temperature for A-60 stone wool on 12 mm steel plate.

The results of this test showed a normal behaviour in the elevation of temperatures, without any apparent issue concerning measurements.

10.3 Analysis of the experimental tests

The analysis of the experimental tests consisted in tracking the highest and average temperature elevations at the non-exposed side of the thermal insulation at the end of the tests. These temperatures were compared with the criteria in the FTP Code:

- Maximum 140 °C average temperature elevation (referred to as criterion AVG)
- Maximum 180 °C peak temperature elevation (referred to as criterion HIGH).

The comparison of temperature elevations is summarized in Table 10.

Table 10. FTP Code requirements compared with temperature elevations in tests with heat exposure according to the hydrocarbon time-temperature curve

Class of thermal insulation	Steel plate thickness (mm)	Peak temperature elevation in tests (°C)	Highest average temperature elevation in tests (°C)	Fire integrity based on HC curve	
				Time (min)	Passed criterion
A-30	6	Test stopped at 8 minutes			
A-60	6	346	286	20	HIGH
A-30	6	503	354	11	AVG
A-30	5	782	687	11	AVG
A-30	12	324	232	17	HIGH
A-60	12	297	236	31	AVG

Without any surprise, the fire integrity based on the HC curve is lower than the fire integrity based on the ISO 834 standard curve.

The test performed with glass wool thermal insulation did not require much analysis. The material melted and shrunk when exposed to the high temperature from the Hydrocarbon time-temperature curve.

Regarding the stone wool thermal insulation, the level of protection was significantly reduced when exposed to the Hydrocarbon time-temperature curve but still presented a certain degree of protection.

Based on the experimental tests, it was possible to calculate the reduction in protection time for standard A-class thermal insulation materials when exposed to the heat from a realistic fire in a ro-ro space, represented by the hydrocarbon time-temperature curve.

10.4 Reduction of A-class insulation protection time

The reduction of the protection time of A-class thermal insulation was calculated as the ratio of the fire integrity based on the hydrocarbon time-temperature curve and the fire integrity based on the cellulosic time-temperature curve used in the FTP Code.

Table 11 shows the reduction in thermal integrity capacity when the A class stone wool insulation was exposed to the hydrocarbon curve.

Table 11. Reduction in fire integrity of A class stone wool thermal insulation exposed to the hydrocarbon time-temperature curve.

Class of thermal insulation	Steel plate thickness (mm)	Fire integrity based on ISO 834 (min)	Fire integrity based on HC tests* (min)	Reduction in fire integrity (HC vs ISO834)
A-60	6	60	20	66%
A-30	6	30	11	60%
A-30	5	30	11	63%
A-30	12	30	17	43%
A-60	12	60	31	48%

The reductions are influenced by the thickness of the steel plate. When steel plate is around 5-6 mm, the reduction was calculated to around 65% but only to 45% when the steel plate is 12 mm thick.

11 Conclusion

Main authors of the chapter: Pierrick Mindykowski (RISE)

The goal of this study was to assess the requirements for horizontal division of ro-ro spaces as well as boundary decks. This was studied by judging if the current required fire integrity (or absence of requirement for internal decks) can sustain a heat exposure from a realistic fire encountered in a ro-ro space. To define such a fire, previously conducted fire tests were analysed and numerical simulations were performed with representative ro-ro spaces (a closed ro-ro space and an open ro-ro space) and representative cargo (full load of HGV). The main result was that only for the case of a completely closed ro-ro space (i.e. no openings at all) and the ventilation turned off, the heat exposure does not exceed the standard time-temperature curve (cellulosic curve or ISO 834) for more than 4 minutes. For other cases i.e. open ro-ro space and closed ro-ro space with ventilation on, the heat exposure is better represented by the hydrocarbon time-temperature curve, which is more severe than the cellulosic time-temperature curve used to test and approve thermal insulation according to the FTP Code.

A series of experiments was carried out to understand how the performance of standard A-class thermal insulation is affected by exposure to the Hydrocarbon time-temperature curve. Thermal insulation consisting of A-30 and A-60 glass and stone wool, were mounted on steel plates with different thicknesses and exposed to the HC curve in a reduced scale furnace. The results showed that the glass wool should be avoided in well-ventilated ro-ro spaces, i.e. ro-ro spaces with openings. Temperature measurements at the unexposed side showed that stone wool gave a reduced level of protection when exposed to the hydrocarbon fire. Moreover, the results showed that the protection time expected of 60 minutes (with A-60 thermal insulation) or 30 minutes (with A-30 thermal insulation) is reduced by 45-60% when exposed to the hydrocarbon heat exposure.

Based on the results presented in this report, ship owners or shipbuilders with the intention to achieve 30 or 60 minutes of passive protection, are recommended to assume a 50% reduction of capacity during exposure and use a higher standard insulation (A-60 if they want to achieve 30 minutes protection) or use insulation of a type approved with the hydrocarbon curve.

12 References

[1] S.-C. o. F. s. Implementation, FSI 21/5 Casuality Statistics and investigation, International Maritime Organization, London, 2012.

[2] IMO, *International Convention for the Safety of Life at Sea (SOLAS), 1974,* London: International Maritime Organization, 1974.

[3] Rahm, M., Evegren,F. (2016) Engineering analysis report of car carrier with FRP decks, SP report.

[4] K. McGrattan, S. Hostikka, J. Floyd, R. McDermott, and M. Vanella. (2020). Fire Dynamics Simulator, User's Guide (NIST Special Publication 1019). National Institute of Standards and Technology.

[5] Fires in Transport Tunnels, EUREKA Project EU 499: FIRETUNE, 1995

[6] H. Ingasson et al., Runehamar Tunnel Fire Tests, SP Report 2011:55, SP Sveriges Tekniska Forskningsinstitut, 2011

[7] M. K. Cheong et al. (2014). Heat Release Rate of Heavy Goods Vehicle Fire in Tunnels with Fixed Water Based Fire-Fighting System. *Fire technology, vol. 50, no. 2*, pp. 249–266.

[8] A. Olofsson *et al.*, Model scale tests of a ro-ro space fire ventilation (RO5 project), 2020.

[9] European Committee for Standardization. (2005). Eurocode 3: Design of steel structures. Part 1-2: General rules. Structural fire design. (EN Standard EN 1993-1-2:2005).

[10] W. Zhang, J. Harff, and R. Schneider, Analysis of 50-year wind data of the southern Baltic Sea for modelling coastal morphological evolution – a case study from the Darss-Zingst Peninsula , *Oceanologia* , vol. 53, no. 1-. Elsevier Urban & Partner Sp. z o.o , SOPOT , pp. 489–518, 2011, doi: 10.5697/oc.53-1-TI.489.

[11] A. Pena Diaz *et al.*, South Baltic Wind Atlas: South Baltic Offshore Wind Energy Regions Project, 2011.

[12] M. Rahimpour and P. Oshkai, Experimental investigation of airflow over the helicopter platform of a polar icebreaker , *Ocean engineering* , vol. 121. Elsevier Ltd, OXFORD , pp. 98–111, 2016, doi: 10.1016/j.oceaneng.2016.05.023.

[13] LASH FIRE, D09.2 Developed ro-ro spaces fire detection solutions and recommendations, 2022.

[14] NUREG-1824 Supplement 1, Verification and Validation of Selected Fire models for Nuclear Power Plant Applications, 2016

13 Indexes

13.1 Index of tables

13.2 Index of figures